



Phytosterols in human serum as measured using a liquid chromatography tandem mass spectrometry

Yu Chun Teng^a, Marie Claire Gielen^a, Nina M de Gruijter^{a,b,c}, Coziana Ciurtin^{b,c},
Elizabeth C. Rosser^{b,c}, Kersti Karu^{a,*}

^a UCL Chemistry Mass Spectrometry Facility, 20 Gordon Street, University College London, London, United Kingdom

^b Centre for Adolescent Rheumatology Versus Arthritis at University College London, University College London Hospital and Great Ormond Street Hospital, London, United Kingdom

^c Centre for Rheumatology Research, Division of Medicine, University College London, London, United Kingdom

ABSTRACT

Phytosterols are lipophilic compounds found in plants with structural similarity to mammalian cholesterol. They cannot be endogenously produced by mammals and therefore always originate from diet. There has been increased interest in dietary phytosterols over the last few decades due to their association with a variety of beneficial health effects including low-density lipoprotein cholesterol lowering, anti-inflammatory and anti-cancerous effects. They are proposed as potential moderators for diseases associated with the central nervous system where cholesterol homeostasis is found to be imperative (multiple sclerosis, dementia, etc.) due to their ability to reach the brain. Here we utilised an enzyme-assisted derivatisation for sterol analysis (EADSA) in combination with a liquid chromatography tandem mass spectrometry (LC-MSⁿ) to characterise phytosterol content in human serum. As little as 100 fg of plant sterol was injected on a reversed phase LC column. The method allows semi-quantitative measurements of phytosterols and their derivatives simultaneously with measurement of cholesterol metabolites. The identification of phytosterols in human serum was based on comparison of their LC retention times and MS², MS³ spectra with a library of authentic standards. Free campesterol serum concentration was in the range from 0.30–4.10 µg/mL, β-sitosterol 0.16–3.37 µg/mL and fucosterol was at lowest concentration range from 0.05–0.38 µg/mL in ten individuals. This analytical methodology could be applied to the analysis of other biological fluids and tissues.

1. Introduction

Plant sterols and plant stanols also referred as phytosterols, are a class of lipophilic compounds found in plants with high structural similarity to cholesterol, a well-known molecule endogenously found in humans, particularly notorious for its relation to cardiovascular disease (CVD) [1–3]. Phytosterols are components of plant membranes, which, like cholesterol, regulate membrane fluidity and permeability [4]. Since phytosterols cannot be endogenously produced by mammals they originate from dietary uptake, food such as in vegetables, fruits, grains, cereals, vegetable oils and margarines [2,5,6]. More than 250 steroids have been described in plants [7–9]. The most frequently occurring plant sterols are β-sitosterols, sitostanol, campesterol and stigmasterol in food and human body [10,11]. Cholesterol averages around 50 mg/kg of total lipid in plants, whereas in mammals it can be as high as 5 g/kg (or more) [12]. The Food and Drug Administration (FDA) and the European Food Safety Authority (EFSA) recognise phytosterols as “safe” and have authorised health claims regarding risk reduction of coronary heart disease with a daily dietary intake of at least 2 g/day [13,14]. This has

led to increased availability and consumption of phytosterol fortified foods and food supplements. The daily intake in a typical western diet averages to about 300 mg for phytosterols and 20 mg for phytostanols [15–17]. However, their absorption efficacies are reported to be much lower >2% and >0.02% for phytosterols and phytostanols respectively. In contrast, the absorption efficiency for cholesterol is estimated at 50–60% [3,18,19].

Sterols are chemically composed of a steroid core consisting of perhydrophenanthrene (A, B and C ring) fused with a cyclopentane (D ring), a hydroxyl group on C3 of the A-ring, a methyl groups attached at C18 and C19, and variable C17-side chain (R) attached to the D-ring (Fig. 1a, b). The difference between distinct sterols lies in the addition of an extra methyl, ethyl or hydroxyl group to the side chain or/and the steroid core. R groups of phytosterols typically contain nine or ten carbons, as opposed to eight in cholesterol [4]. In contrast to plant sterols, plant stanols contain a saturated core. (Fig. 1d). Phytosterols can occur free forms and in four conjugated forms in which the hydroxyl group at C3 is esterified with a fatty acid (FA) or hydroxycinnamic acid (HA) and glycosylated to a hexose (GH) or acyl hexose (AGH) (Fig. 1c).

* Corresponding author.

E-mail address: kersti.karu@ucl.ac.uk (K. Karu).

<https://doi.org/10.1016/j.jsbmb.2024.106519>

Received 16 February 2024; Received in revised form 5 April 2024; Accepted 9 April 2024

Available online 12 April 2024

0960-0760/© 2024 The Authors. Published by Elsevier Ltd. This is an open access article under the CC BY license (<http://creativecommons.org/licenses/by/4.0/>).

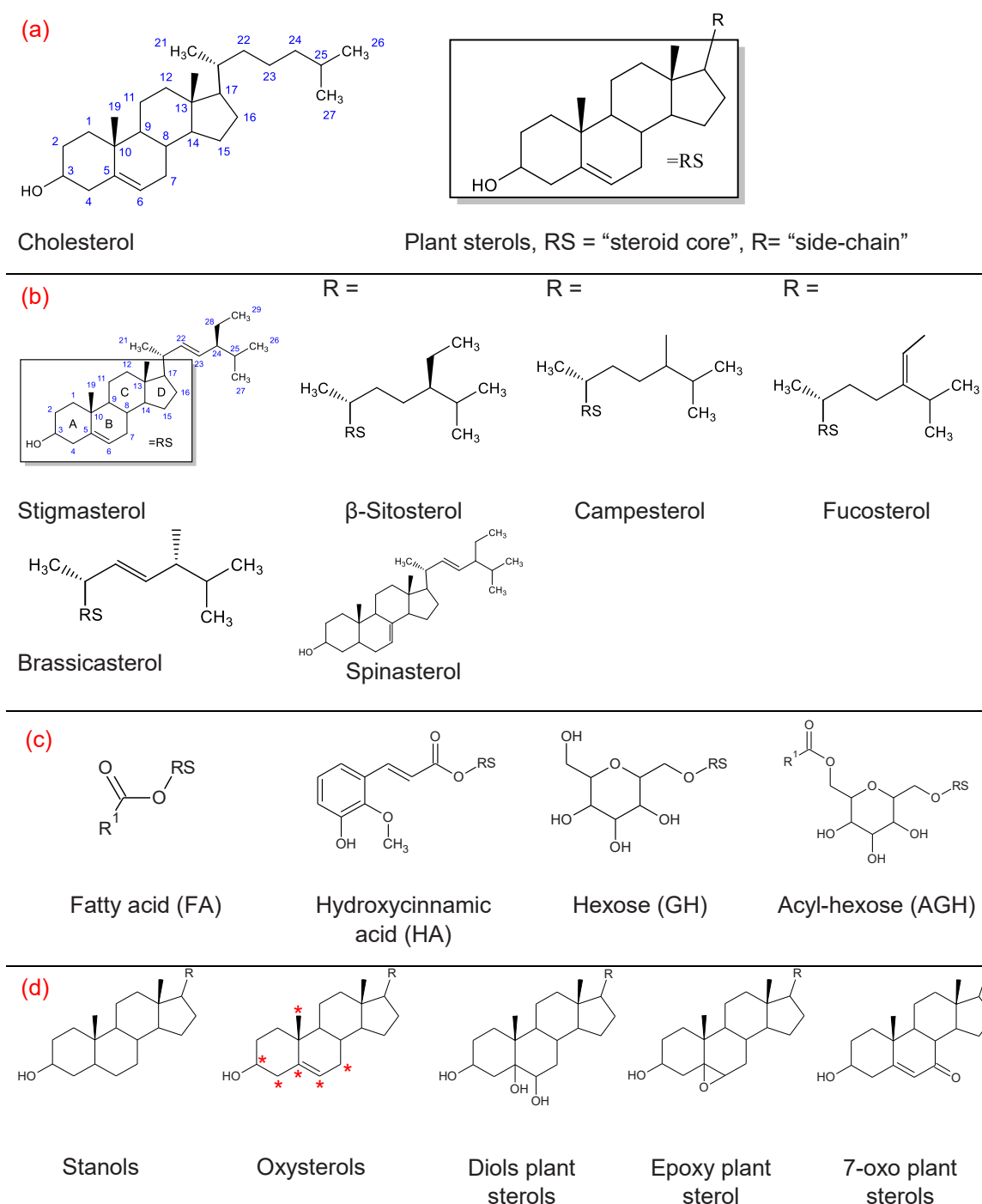


Fig. 1. Chemical structures of plant sterols and their derivatives. (a) Basic structure of sterol with respective numbering. Most phytosterols (PS) have the same steroid core (A, B, C, D rings). The R group is a carbon side-chain. (b) The most abundant phytosterols:- campesterol, β -sitosterol, brassicasterol, fucosterol, stigmasterol and spinasterol. (c) The four main conjugates of PS. The hydroxyl group at C3 is esterified to a fatty acid (FA), where R1 is the carbon chain of the fatty acid or hydroxycinnamic acid (HA) or glycosylates to a hexose (HA) or acyl-hexose (AGH). The C3 hydroxyl group of HA is esterified to ferulic acid (here shown) or p-coumaric acid and AGH has a fatty acid that is esterified to the 6-OH of the hexose moiety. (d) Plant stanols, which contain a saturated core, also possible oxidation points on (plant) sterols are shown by asterisk and examples of diols, epoxy, and 7-oxo (plant) sterols.

Phytosterols and cholesterol can be oxidised to oxyphytosterols and oxysterols respectively (Fig. 1d). Oxyphytosterols are present in low levels in food but are tentatively endogenously produced in humans following intestinal absorption by similar biochemical pathways as oxysterols [4,13,14,20]. Both cholesterol and phytosterols are prone to autoxidation under conditions such as heat and light during food processing, or by reactive oxygen species in tissues [21,22]. Oxyphytosterols in food such as 7-oxo, 7-hydroxy-, and 5,

6-epoxy-phytosterols are autoxidised on the sterol-ring (Fig. 1d), while side-chain oxidation is mediated by specific enzymes [3,14]. For example, 24-hydroxycholesterol and 27-hydroxycholesterol are hydroxylated by cytochrome P450 oxidase CYP46A1 and CYP27A1, respectively. Plat J reported an average serum cholesterol concentration in the general population around 5 mmol/L, whereas concentrations of plant sterols by 400 times lower and stanols by 100,000 times lower than cholesterol [14].

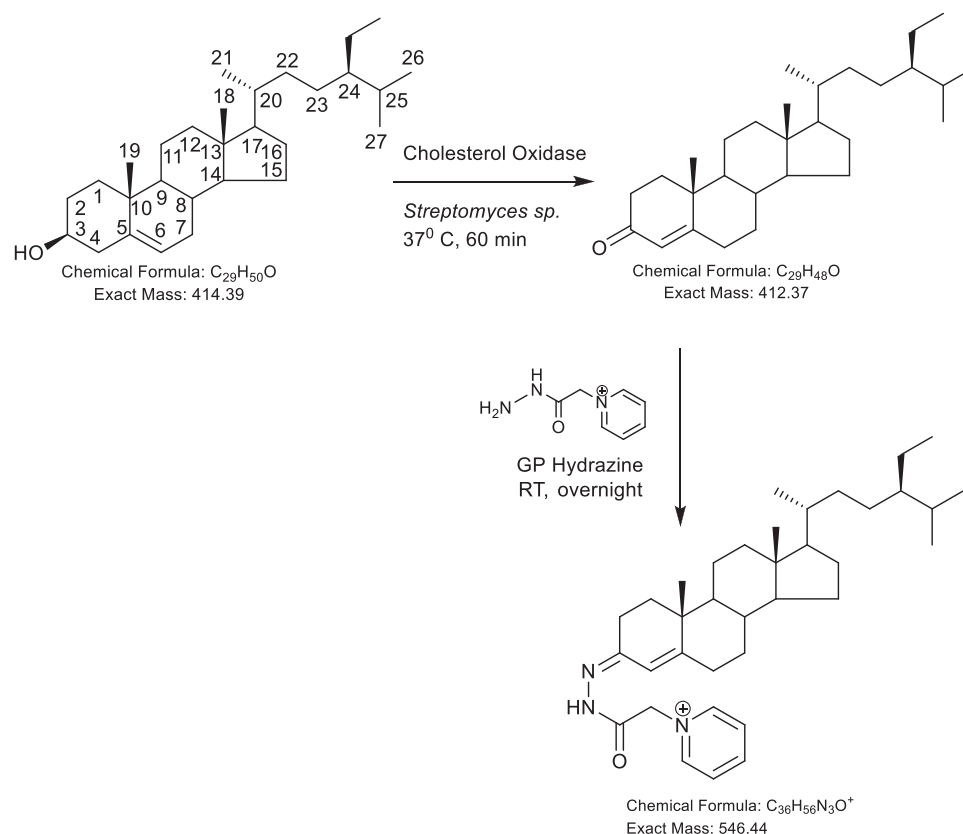


Fig. 2. Enzyme-assisted derivatisation for sterol analysis EASDA. Example is shown for β -sitosterol, of which 3 β -hydroxy group was converted to 3-oxo group using cholesterol oxidase enzyme from *Streptomyces sp.* followed by Girard P (GP) reagent derivatisation to GP hydrazone, O/GP β -sitosterol.

Over 20 % of free cholesterol in humans is found in the brain, where steady cholesterol homeostasis is essential for proper functioning of neurons [23]. Cholesterol biosynthesis and metabolism is tightly regulated in the central nervous system (CNS) [24,25]. Pathophysiological studies have linked disturbed metabolism of cholesterol to neurological and neurodegenerative diseases such as multiple sclerosis, Alzheimer's disease, and dementia [1,2,10,14]. Phytosterols have been proposed to have therapeutic effects in the pathogenesis of neurodegenerative diseases, potentially by modulating cholesterol homeostasis in CNS [26,27]. As phytosterols have been supplemented in functional food products, this leads to increase dietary exposure of both phytosterols and their oxidation products [3,12,28]. Recent studies show that phytosterols and oxyphytosterols can traverse the blood brain barrier (BBB) and accumulate in the brain [13,20]. Based on this finding, researchers have started to investigate the physiological role of phytosterols and their oxidation products [13,20].

Many methodologies were exploited to analyse phytosterols in biological samples, from the traditional methods using thin-layer chromatography (TLC), to liquid chromatography (LC) [11,13,29,30]. Nowadays, phytosterols and their oxidation products analyses are dominated by GC-MS using selected-ion monitoring (SIM) or LC-MS/MS method combined with multiple reaction monitoring (MRM) [31,32]. In summary, the protocol usually starts with the addition of ethylenediamine tetraacetic acid (EDTA) and butylated hydroxytoluene (BHT) to minimise autoxidation of sterols, following by alkaline hydrolysis to unesterified sterols. For measuring only free sterols, hydrolysis is omitted. This follows by solid-phase extraction (SPE) using either a reversed- or normal-phase SPE cartridges. Sterols are then derivatised to their trimethylsilyl ester (TMS) derivatives to enhance volatility prior to GC-MS analysis [29,33,34]. The LC-MS/MS analyses are current popular choice [35]. To enhance sensitivity of measurements and phytosterol solubility, different derivatisation agents were used to transform sterols

to their picolinyl ester-, [36] nicotinyl esters-, [37] and Girard P (GP) hydrazones [29,38,39].

Here, we utilised an enzyme-assisted derivatisation for sterol analysis (EASDA) technology for measurement of non-esterified free phytosterols in human serum. EASDA is a chemical approach, where 3 β -hydroxy-5-ene or 3 β -hydroxy-5 α -hydrogen sterols convert to 3-oxo-4-ene or 3-oxo sterols using cholesterol oxidase from *Streptomyces sp.* The sterols possessing an oxo group are then derivatised with the commercially available Girard P reagent (Fig. 2). The derivatisation reaction with the Girard P hydrazine is carried out directly on the products of the cholesterol oxidase reaction, without any further purification or extraction. The incorporation of the GP hydrazone group into the 3-oxo sterol structure increases the mass of the sterol by 134 Da. The resulting GP hydrazones are then separated from excess GP hydrazine using a recycling protocol on a reversed phase SPE cartridge. The benefits of EASDA are: - (a) sterols solubility increase, and (b) enhancement in an electrospray (ES) signal by 1000 in comparison to underivatized sterols versions [40,41]. Most importantly, sterol GP-hydrazones generate informative MS³ ($[M]^+ \rightarrow [M-79]^+ \rightarrow$) spectra benefiting their structural elucidation [42,43]. We analysed the resulting samples using a capillary LC coupled to a linear ion trap mass spectrometer.

2. Materials and methods

2.1. General

High-performance liquid chromatography (HPLC)-grade water, absolute ethanol, and other HPLC-grade solvents were from Fisher Scientific (Loughborough, UK) or Sigma-Aldrich (Dorset, UK). Acetic acid was AnalaR NORMAPUR grade (BDH, VWR, Lutterworth, UK). Cholesterol (5-cholesten-3 β -ol), cholestanol (5 α -cholestan-3 β -ol), lathosterol (7,5 α -cholesten-3 β -ol), desmosterol (5,24-cholestadien-3 β -ol), fucosterol (5-

cholesten-24(28)-ethylidene-3 β -ol), campesterol (5-cholesten-24-methyl-3 β -ol), β -sitosterol (5-cholesten-24 β -ethyl-3 β -ol), stigmasterol (5,22-cholestadien-24 β -ethyl-3 β -ol), brassicasterol (5, 22-cholestadien-24 β -methyl-3 β -ol), 7-keto- β -sitosterol (5-cholesten-24-ethyl-3-ol-7-one), and [25,26,26,26,27,27,27-²H₇] cholesterol ([25,26,26,26,27,27,27-²H₇] C²⁵-3 β -ol) were purchased from Steraloids, Inc. (Newport, R.I., USA). All reference sterols were stored at -20°C. Desmosterol was wrapped in foil because of its sensitivity to light. Cholesterol oxidase from *Streptomyces* sp. was from Sigma-Aldrich (Dorset, UK). Girard P (GP) reagent (1-(carboxymethyl)pyridinium chloride hydrazide) was from Santa Cruz Biotechnology, Inc. Certified Sep-Pak C₁₈ SPE cartridges (3 cc, 200 mg) were from Waters (Elstree, UK). Luer-lock syringes were from BD Biosciences (Sigma-Aldrich). Glacial acetic acid (99.9 %) was from Sigma-Aldrich (Dorset, UK). Formic acid (LC-MS grade) was from Fisher Scientific, Inc. (Loughborough, UK). HPLC grade chloroform, dichloromethane, propan-2-ol and ethanol and LC-MS grade methanol, water and acetonitrile were from Honeywell, Fisher Scientific and/or VWR. Potassium phosphate monobasic (KH₂PO₄, \geq 99.5 %) was from Honeywell (Seelze, Germany). All necessary plastic materials used were as described in [44].

2.2. Human serum samples

The blood samples were collected from six healthy volunteers of age 23–30, three females and three males, with BMI 18–22 during public engagement events (including young scientist days) organised by the Center for Adolescent Rheumatology Versus Arthritis, Division of Medicine, University College London (UCL). Two blood samples were collected from patients with Juvenile Onset Systemic Lupus Erythematosus (JSLE) attended the adolescent and young adult lupus clinics at University College London Hospital, females ages 20 and 26 with BMI 20. Two samples were from patients with alternating hemiplegia of childhood (AHC), female and male age 33, BMI 22. Informed written consent or parental consent/participant assent was acquired from both patients and healthy volunteers as age-appropriate under the ethical approval reference: REC11/LO/0330 and in accordance with the Declaration of Helsinki. All information was stored as pseudo-anonymised data. Blood serum was used for mass spectrometry analyses. The blood serum samples were collected in serum gel S/9 monovette® (Sarstedt). Serum was separated from blood cells by centrifugation at 3500 rpm for 10 min at 18 °C (Heraeus multifuge 4KR centrifuge, Osterode, Germany). To avoid autoxidation 10 μ L of a methanolic butylated hydroxytoluene (BHT 25 mg/mL) solution was added to 1 mL serum.

2.3. Enzyme-assisted derivatisation (EADSA)

Authentic standards of phytosterols were dissolved in ethanol to make 1 μ g/ μ L stock solutions. Next, 2 μ L of stock solution was added into 98 μ L of propan-2-ol in a 5 mL round-bottom flask followed by addition of phosphate buffer solution (1 mL, 50 mM KH₂PO₄, pH 7) containing 3 μ L cholesterol oxidase from *Streptomyces* sp. (2 mg/mL, 44 units/mg). The mixture was incubated at 37 °C for 60 min to convert 3 β -hydroxy-5-ene moiety to 3-oxo-4-ene. The oxidation was quenched with 2 mL methanol. Glacial acetic acid (150 μ L) and GP hydrazine (150 mg) were added. The mixture was left overnight to derivatise 3-oxo-4-ene sterols to GP hydrazones.

2.4. Recycling solid phase extraction

Recycling SPE was carried out to remove excess GP reagent as previously published [21,44]. A 200 mg Sep-Pak Vac cartridge was washed with 6 mL 100 % methanol, followed by 6 mL 10 % methanol, and then conditioned with 4 mL 70 % methanol. The GP reaction mixture (3.25 mL in 70 % methanol) after oxidation and GP derivatisation procedures was directly applied on the C₁₈ SPE cartridge, followed by 1 mL of 70 % methanol (this is a wash of the reaction vessel), and 1 mL of

35 % methanol. The effluent was collected into a glass beaker. The combined effluent (now 5.25 mL) was diluted with 4 mL of water. The resulting mixture (now 9 mL in 35 % methanol) was again applied to the C₁₈ SPE column, followed by a wash with 1 mL of 17 % methanol. The effluent was collected into the glass beaker. To the combined effluent, 9 mL of water was added to give 19 mL of about 17.5 % methanol. This was again applied to the C₁₈ SPE column and the effluent was discarded. At this point, most GP-hydrazones were retained on the C₁₈ cartridge. The cartridge was then washed with 6 mL 10 % methanol in water to remove excess of GP hydrazine. Our validation experiments confirm the required volumes of elution solvents required to elute fully derivatised phytosterols (Appendix A). We found that cholesterol- and phytosterol-GP-hydrazones eluted with three 1-mL portions of 100 % methanol and collected in 1.5 mL-microcentrifuge tubes (SPE-2-Fr1, 2, 3), followed by four 1-mL portions of 100 % ethanol (SPE-2-Fr-4, 5, 6, 7) and another application of two 1-mL portions of 100 % DCM (SPE-2-Fr-8, 9) from the SPE-2 C₁₈ cartridge.

2.5. Extraction of phytosterols from human serum

One hundred μ L of serum was added drop-wisely into a 2-mL Eppendorf tube containing 1 mL of absolute ethanol and 0.5 μ L of [²H₇] cholesterol (2 μ g/ μ L in propan-2-ol). The sample was sonicated for 5 min. Then, 330 μ L of water was added to the tube and ultrasonicated for a further 5 min, and the sample was then centrifuged at 14,000 \times g at 4°C for 30 min. The resulting sample contained 70 % ethanol. A 200-mg Sep-Pak C₁₈ cartridge was rinsed with 4 mL of ethanol and then conditioned with 6 mL of 70 % ethanol. We adapted a previously published protocol [42] where authors validated the method with a solution of cholesterol and 24(R/S)-[26,26,26,27,27,27-²H₆] hydroxycholesterol in 70 % ethanol, they found that cholesterol was retained on the column even after a 5.5-mL column wash of 70 % ethanol, whereas 24(R/S)-[26,26,26,27,27,27-²H₆] hydroxycholesterol elutes in the flow-through and column wash. They also mentioned that after a further column wash with 4 mL of 70 % ethanol, cholesterol was eluted from the column in 2 mL of absolute ethanol. They further applied an additional 2 mL of absolute ethanol on the column to elute more hydrophobic sterols. Therefore, in this work, the flow-through (1.43 mL) and a column wash of 9.5 mL of 70 % ethanol were collected in a 15 mL round-bottom flask to elute more polar phytosterols from the column (Figure S1). As some phytosterols are more lipophilic than cholesterol, we eluted them in 8 mL ethanol (Figure S1, fraction B). Just mention here we applied sequentially 1 mL of ethanol eight times on the cartridge. The cartridge was further stripped with 2 mL DCM to elute even more lipophilic phytosterols (Figure S1, fraction C). All three fractions were combined into the same round-bottom flask. Finally, the solvent was dried using a rotary evaporator. Then the samples were reconstituted with 100 μ L propan-2-ol and thoroughly vortexed, before they were subjected to cholesterol oxidation, GP-derivatisation and SPE-2 on a C₁₈ column, as described above.

2.6. Direct infusion single-stage TOF-MS

A Premier XE Q-TOF-MS connected to a 2777 C autosampler (Waters, UK) was utilised to screen SPE-2 fractions for each sample. The ESI was operated in positive mode. The capillary voltage was 2.5 kV and sample cone voltage was 50 V. The desolvation and source temperatures were 150 °C. The desolvation gas flow was 450 L/h and the cone gas flow was 100 L/h. The mass range was m/z 100–800 and the scan rate was 1 s⁻¹. Samples (10 μ L) were directly infused in 50 % of mobile phase A (MeOH, Propan-2-ol, Formic acid 50:50:0.1, v/v/v) and 50 % mobile phase B (MeOH, Formic acid 100:0.1, v/v/v) with a flow of 0.2 mL/min. The analysis time was 2 minutes. Then, one fraction for each the O/GP derivatised phytosterol with the highest [M]⁺ signal was selected for a LC-MSⁿ analysis.

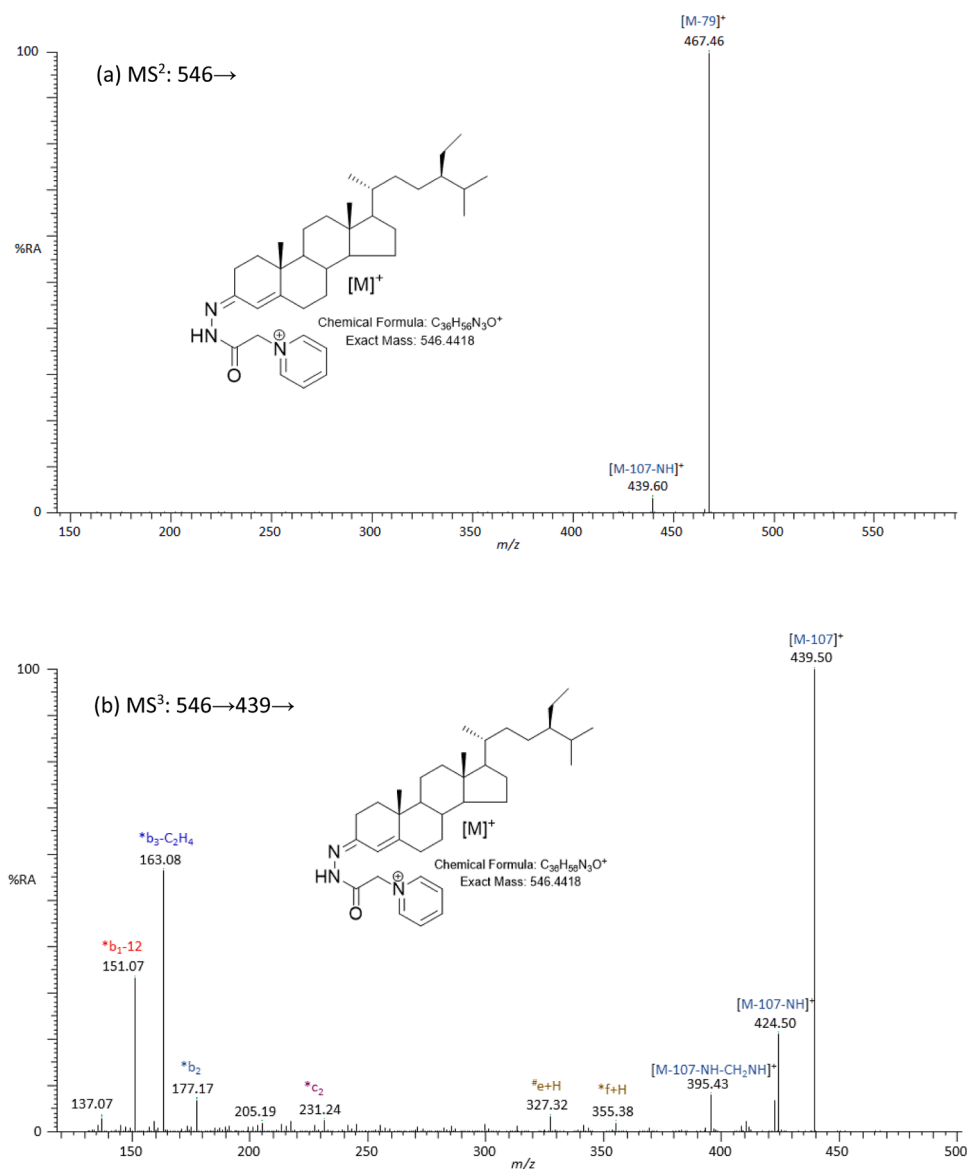


Fig. 3. (a) ES- MS^2 (546→); and (b) MS^3 (546→439→) spectra of the oxidised and GP-derivatised β -sitosterol authentic standard.

2.7. Direct infusion ES multi-stage fragmentation mass spectrometry

A Thermo Finnigan LTQ linear ion trap mass spectrometer (Thermo Fisher Scientific, UK) was operated with the following settings: - spray voltage 1.00–1.20 kV, capillary temperature 200^o C, no sheath or auxiliary gas used. The mass range m/z 50 – 700 was scanned, and centroid data was collected. MS, MS^2 and MS^3 spectra were recorded. MS^2 experiment was performed on a precursor ion. MS^2 spectra were dominated by $[M-79]^+$ and $[M-107]^+$ fragment ions. MS^3 scans were performed on fragment-ions resulting from a neutral loss of 79 Da or 107 Da in the MS^2 . For acquisition of both MS^2 and MS^3 spectra, the collision energy setting was 35 % with the isolation width at 1.00. MS, MS^2 and MS^3 scans consisted of three averaged micro scans each with a maximum injection time of 200 ms.

2.8. Capillary-LC-ES- MS^n

LC- MS^n analyses were performed using an Accela HPLC system interfaced to the LTQ MS. The LC system is comprised of an autosampler, degasser and pump system. The injection volume was 10 μ L. Chromatographic separation was achieved on a Hypersil Gold C₁₈ column

(1.9 μ m particles, 100 mm×21 mm, Fisher Scientific). Mobile phase A was composed of 33.3 % methanol, 16.7 % acetonitrile, with 0.1 % formic acid and mobile phase B was 60 % methanol, 40 % acetonitrile, 0.1 % formic acid. Initially B was at 50 % and was raised to 70 % over 3 min, then was raised to 99 % B over the next 17 min and stayed at 99 % B for 3 min, before returning to 50 % B in 6 s and re-equilibrating for a further 5 min 54 s, giving a total analysis time 26 min. The flow rate was 180 μ L/min. The eluent was directed to the ESI source of the LTQ mass spectrometer. The ESI was operated in positive mode with a capillary temperature of 280 o C. The spray and capillary voltages were set to 4.5 kV and 33 V respectively. The sheath, auxiliary and sweep gas flow rates were 40, 10 and 0 respectively. The ion trap analyser set-up for seven scan events during one LC-MS analysis. In event 1 full scan of m/z 80–600, then follows by other 6 events set either for MS^2 and/or MS^3 scans. MS^2 transition was set on an expected derivatised phyto-sterols or predicted their metabolites/autoxidation products. The MS^3 scans were performed on fragment-ions resulting from a neutral loss of 79 Da and 107 Da in the MS^2 , $[M]^+ \rightarrow [M-79]^+ \rightarrow$, and $[M]^+ \rightarrow [M-107]^+ \rightarrow$. A precursor-ion include list for and MS^3 $[M]^+ \rightarrow [M-79]^+ \rightarrow$, transitions for potential oxyphyto-sterols were set-up. MS^1 , MS^2 and MS^3 scans contain three averaged microscans, each with a maximum ion fill

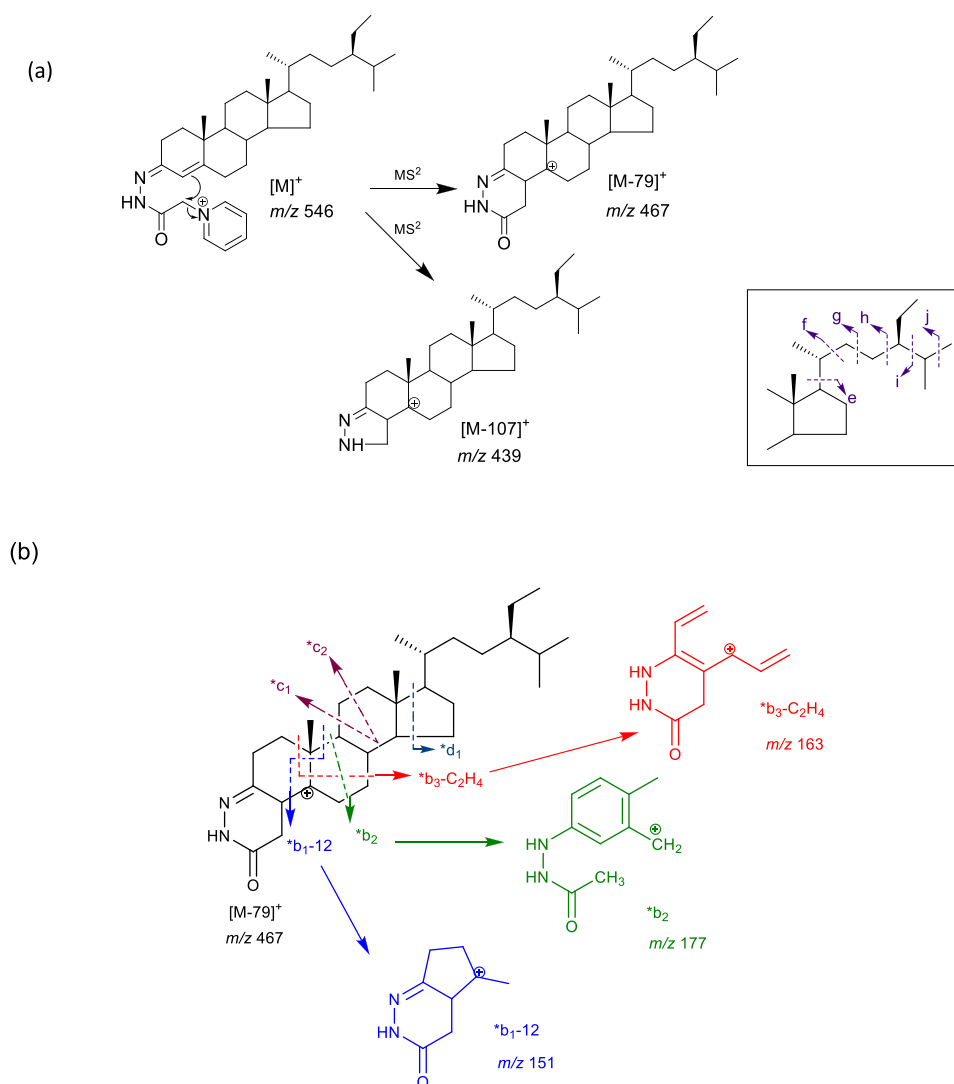


Fig. 4. (a) MS² fragmentation, (b) MS³ ($[M]^+ \rightarrow [M-79]^+ \rightarrow$) fragmentation of the O/GP-derivatised β -sitosterol. An asterisk preceding a fragment-ion describing letter e.g. $*b_1-12$, indicates that the fragment-ion has lost the pyridine moiety from the derivatising group. A prime to the left of a fragment ion describing letter e.g. $*f$, indicates that cleavage proceeds with the transfer of a hydrogen atom from the ion to the neutral fragment. A prime to the right of the fragment describing letter indicates that cleavage proceeds with hydrogen atom transfer to the fragment-ion e.g. $*e'$. The inset indicates fragmentation in the C-17 side chain of the GP-derivatised sterols. Figures were taken from [21,41,44,47] with permission.

time of 200 ms. For MS² and MS³ the isolation width was set to 1 m/z for the selection of precursor-ions and the normalised collision energy was 35 %. For the analysis of GP-tagged phytosterols in serum, 10 μ L of each SPE-2 fraction were combined and further diluted with 180 μ L of mobile phase A and 180 μ L of mobile phase B. For analysis of oxysterols/oxysterols, 46.65 μ L of the combined SPE-2 fractions (SPE-2-Fr1 to 7) was diluted with 28.35 μ L of ACN, 25 μ L 0.1 % FA in water. Each SPE-2 fraction was also analysed separately, and the sample for injection was prepared as follows 46.65 μ L of each SPE-2-fraction diluted with 28.35 μ L of ACN, 25 μ L 0.1 % FA.

3. Results and discussion

3.1. Mass measurement of authentic standards

Griffiths and colleagues [21,24,44–46] developed EADSA technology for sterols analysis which was adapted in this research. Briefly, cholesterol, its precursor desmosterol ($C^{5,24}$ - β -ol), and the plant sterols stigmasterol (24 β -ethylcholesta-5,22-dien-3 β -ol, $C^{5,22}$ -24 β -ethyl-3 β -ol), sitosterol (24 β -ethylcholest-5-en-3 β -ol, C^5 -24 β -ethyl-3 β -ol), campesterol

(24 β -methylcholest-5-en-3 β -ol, C^5 -24 β -methyl-3 β -ol), and brassicasterol (24 β -methylcholesta-5,22-dien-3 β -ol, $C^{5,22}$ -24 β -methyl-3 β -ol) were oxidised with cholesterol oxidase and derivatised with GP reagent. Cholesterol oxidase converts 3 β -hydroxy-5-ene sterols to their 3-oxo-4-ene analogs, and the resulting 3-oxo group derivatised with GP hydrazine giving 3-GP hydrazones. The GP authentic standards were directly infused into the linear ion trap MS, and the MS¹, MS² and MS³ spectra were recorded and established as the reference library. These GP hydrazones give intense $[M]^+$ ion signal upon ESI ionization. For example, O/GP-derivatised β -sitosterol gives a $[M]^+$ ion at m/z 546. The MS² (546 \rightarrow) spectrum shows $[M-79]^+$ ions at m/z 467 and $[M-107]^+$ at m/z 439 (Fig. 3a). The MS³ (546 \rightarrow 467 \rightarrow) spectrum contains a triad of fragment ions at m/z 151, 163, 177 (Fig. 3b). A similar triad of fragment ions is observed in the MS³ ($[M]^+ \rightarrow [M-107]^+ \rightarrow$) spectrum, but with the fragment ions displaced in mass by 28 Da, corresponding to additional loss of CO (data not shown). These fragment ions are characteristic of the derivatised 3-oxo-4-ene structure in the absence of additional groups in the A and B rings. They are formed by cleavage in the B-ring and are described by two competing series of b-type fragment ions (Fig. 4). The $*b$ ion-series corresponds to B-ring fragment ions which have formed via

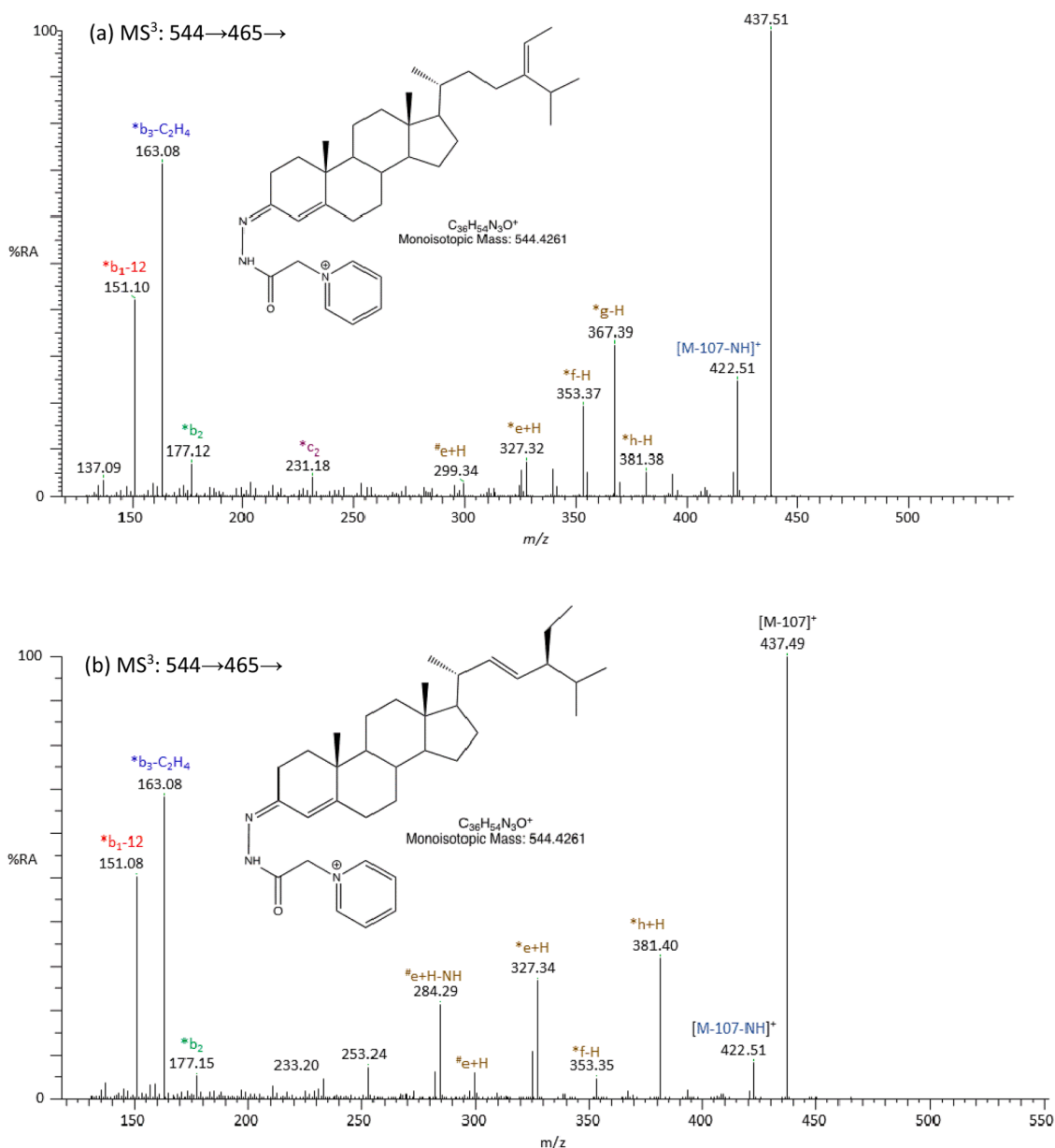


Fig. 5. The MS³ (544→465→) spectra for (a) O/GP fucosterol, and (b) O/GP stigmasterol authentic standards.

the [M-79]⁺ intermediate (which corresponds to the precursor ion having lost the pyridine ring). The *b ion-series of fragment ions are generated in the MS³ [M]⁺→[M-79]⁺ spectra. These fragment ions are described as *m/z* 151 (*b₁-12), 163 (*b₃-C₂H₄) and 177 (*b₂) (Fig. 4) [24,41,44–47].

A library of fragmentation patterns MS² and MS³ spectra for sterol GP hydrazones has been established and could be used by researchers for the structure elucidation of GP-tagged sterols [21,24,45,46,48]. In summary, the *b and #b ion-series are indicative of the sterols possessing a 3-oxo-4-ene group before GP derivatisation and a 3β-ol-5-ene structure before treatment with cholesterol oxidase and GP reagent, with no additional substituents in the A and B rings. This pattern changes with the introduction of hydroxy- or oxo-groups in the B rings of sterols.

While the major cleavages in the sterol ring system occur in the B-ring and give abundant fragment ions, minor but important fragment ions are generated by cleavages in the C- and D-rings, and in the C-17 side-chain giving the fragment ions of low abundance in MS³ spectra. In the MS³ ([M]⁺→[M-79]⁺) spectrum for GP-derivatised fragment ions *c₂, *d₁, #e+H (#e'), and *e+H (*e') are consistently observed at *m/z*

231, 285, 299, 327 for O/GP-derivatised cholesterol, desmosterol, and campesterol (Figures. S3–S5) [41]. Desmosterol is an intermediate in the *de novo* synthesis of cholesterol. MS³ ([M]⁺→[M-79]⁺) of gives a similar spectrum to those other 3-oxo-4-ene sterols. However, peaks at 353 and 355 corresponding to *f-H (*f) and *f+H (*f'); and 325 and 327 corresponding to #e-H (#e) and #e+H (#e'), are of elevated intensity. These ions are formed by cleavage of the bond between C-20 and C-22.

The MS³ spectra of the O/GP-derivatised stigmasterol (24β-ethylcholesta-5,22-dien-3β-ol), β-sitosterol (24β-ethylcholest-5-en-3β-ol), campesterol (24β-methylcholest-5-en-3β-ol), and brassicasterol (24β-methylcholesta-5,22-dien-3β-ol) showed the common features of 3-oxo-4-ene sterol GP hydrazones fragmentation of the B-ring. The MS³ ([M]⁺→[M-79]⁺) spectrum of O/GP-β-sitosterol was similar to cholesterol (Fig. 3b, Figure S2). However, the peak at 367 in the spectrum of cholesterol (Figure S3c) corresponding to the doubly unsaturated cholestane carbonium ion, shifted to 395, and shifted to 381 in the MS³ spectrum of the O/GP-derivatised campesterol (Figure S5c). The peak at *m/z* 424 is a loss of C₃H₆ from the side-chain. The MS³ spectrum of the GP-derivatised stigmasterol is characterised by peaks at 381

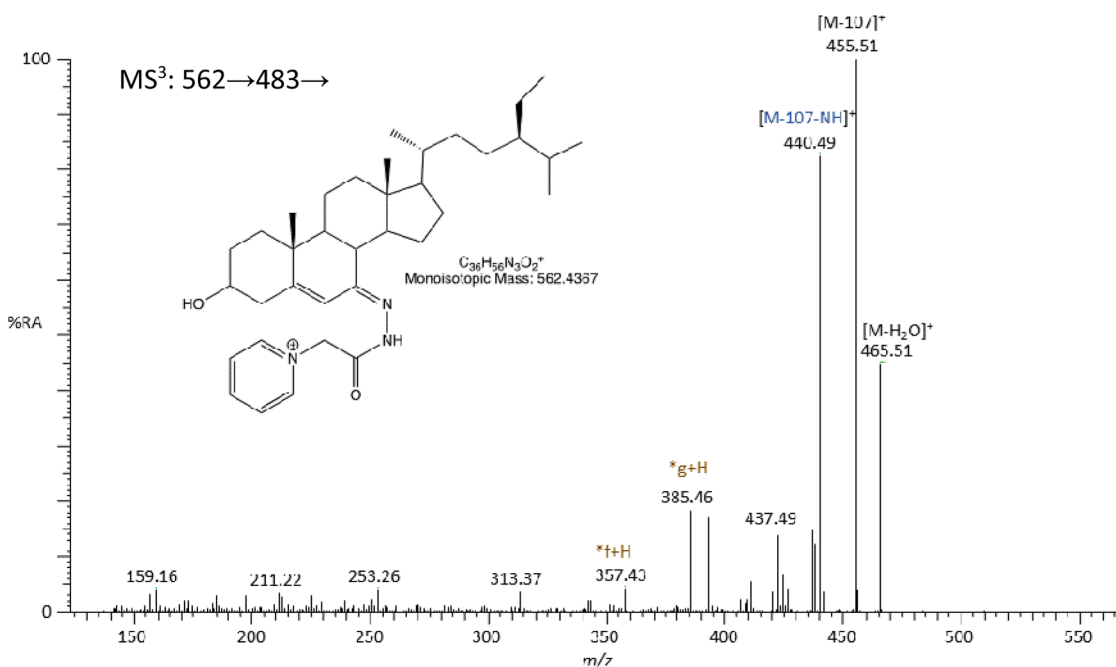


Fig. 6. (a) MS³ (562.5→483.5→) spectrum of O/GP 7-oxo- β -sitosterol authentic standard.

(*h+H) both formed because of cleavage of the C-23-C-24 bond (Figure S6). There is also enhanced abundance of fragment ions at m/z 284 ([#]e'-NH), 299 ([#]e'), and 327 (^{*}e') each formed because of cleavage of the C-17-C-20 bond. The presence of methyl group, rather than an ethyl group, attached to C-24 in brassicasterol leads to the same ^{*}e' and ^{*}h' fragment ions (Figure S7).

The GP derivatised fucosterol and stigmasterol have the same elemental composition (both m/z 544) and were indistinguishable by MS² spectra (544→). However, MS³ (544→465→) of the GP derivatised fucosterol MS³ spectrum shows the C₁₇ side-chain fragment ions at m/z 367 (^{*}g-H) and m/z 353 (^{*}f-H) with of significant intensities (Fig. 5a). Whereas stronger signal of m/z 381 (^{*}h+H), m/z 327 (^{*}e+H) and m/z 284 ([#]e+H-NH) were observed for the GP derivatised stigmasterol (Fig. 5b).

7-Oxo- β -sitosterol was derivatised by GP hydrazine at C-7 position even though it was oxidised by cholesterol oxidase enzyme during our sample preparation, giving the peak at m/z 562 (Supplemental Fig. 7a). In contrast to 3-oxo compounds, 7-oxo compounds showed a prominent pattern of fragmentation ions corresponding to [M-97-H₂O]⁺, [M-107-NH]⁺ and [M-107]⁺. The MS³ spectrum (562→483→) of the GP derivatised 7-oxo- β -sitosterol give a minor fragmentation at m/z 157/159, which probably consists of the unsaturated diazacyclohexanone ring and remnants of the B-ring.

MS³ ([M]⁺→[M-79]⁺) spectra, both O/GP-derivatised cholestanol and lathosterol showed a strong signal at m/z 413 and 411 corresponding to [M-107]⁺ ions, and intensities of other fragment ions were low (RA<10%), and giving limited structural information. In MS³ (520.5→441.5→) spectrum of the O/GP derivatised cholestanol showed only two fragment-ions above RA of 10% at m/z 413 and 398 corresponding to [M-107]⁺ and [M-107-NH]⁺ (Fig. 7a) Therefore, MS⁴ ([M]⁺→[M-79]⁺→[M-107]⁺) spectrum were recorded (Fig. 7b). MS⁴ (520.5→441.5→413.5→) spectrum shows a prominent [M-107-CH₂NH]⁺ fragment-ion at m/z 384 and m/z 369 corresponding to the ([M-107-NH-CH₂NH]⁺) fragment-ion, which are a partial loss of GP derivative and a typical fragmentation of steroid backbone. The MS, MS², MS³ spectra for other studied authentic standards including some oxysterols summarised in Figures S2 to S17.

3.2. Chromatographic separation of O/GP derivatised authentic standards phytosterols

Several capillary LC-MS methods were tested and summarised in Appendix A. Fig. 8 shows a chromatographic separation of O/GP authentic standards on the C₁₈ column using the finalised gradient of 26-min. The O/GP lathosterol and cholesterol with 8-carbons saturated sidechain at C17 co-eluted at RT 7.38, cholestanol eluted at RT 7.39 min from the reversed phase column. The O/GP campesterol with 9-carbons sidechain at C17 eluted at RT 7.75 min and β -sitosterol with 10-carbons sidechain at C17 eluted at RT 8.28 min. The location of the double bond in the side chain also influences the retention on the reversed phase. For example, the O/GP desmosterol with 8-carbons sidechain at C17 eluted at RT 6.49 min, brassicasterol with 9-carbons in the sidechain eluted at RT 7.33 min, whereas fucosterol as well as stigmasterol have 10-carbons in the unsaturated sidechain at C17 eluted at RTs 7.42 min and 7.88 min, respectively. The O/GP cholesterol and lathosterol co-eluted on the LC column using the 26-min gradient. However, the MS³ spectrum of the O/GP lathosterol shows a characteristic fragment-ion at m/z 159, which is not present in the MS³ spectrum of cholesterol (Figure S10c). The separation of the *syn*- and *anti*-conformers was also achieved for the O/GP campesterol, brassicasterol and β -sitosterol (Fig. 8). In general, the longer the sidechain the greater the retention time and the introduction of a double bond in the side chain reduces retention time. Also, the location of hydroxy- or keto-groups in the B-ring and/or in the sidechain decrease the retention times. For example, the O/GP 7 α ,25-dihydroxycholesterol eluted at RT 4.51 and 5.08 min *syn*- and *anti*-conformers, 7 α ,27-dihydroxycholesterol at RT 4.82 and 5.49 min *syn*- and *anti*-conformers, 25-hydroxycholesterol at 6.03 min, 7-oxo- β -sitosterol eluted at 6.12 min, 27-hydroxycholesterol 6.33 min and 6.58 min *syn*- and *anti*-conformers from the C₁₈ column. The chromatographic separation was also achieved for the O/GP 7 β -hydroxycholesterol RT 8.98 and 9.92 min *syn* and *anti*-conformers, 7 α -hydroxycholesterol RT 10.19 and 11.29 min *syn*- and *anti*-conformers using the 26-min gradient (Figure S19). The calibration curves and a limit of detection (LOD) and limit of quantification (LOQ) are presented in Appendix A.

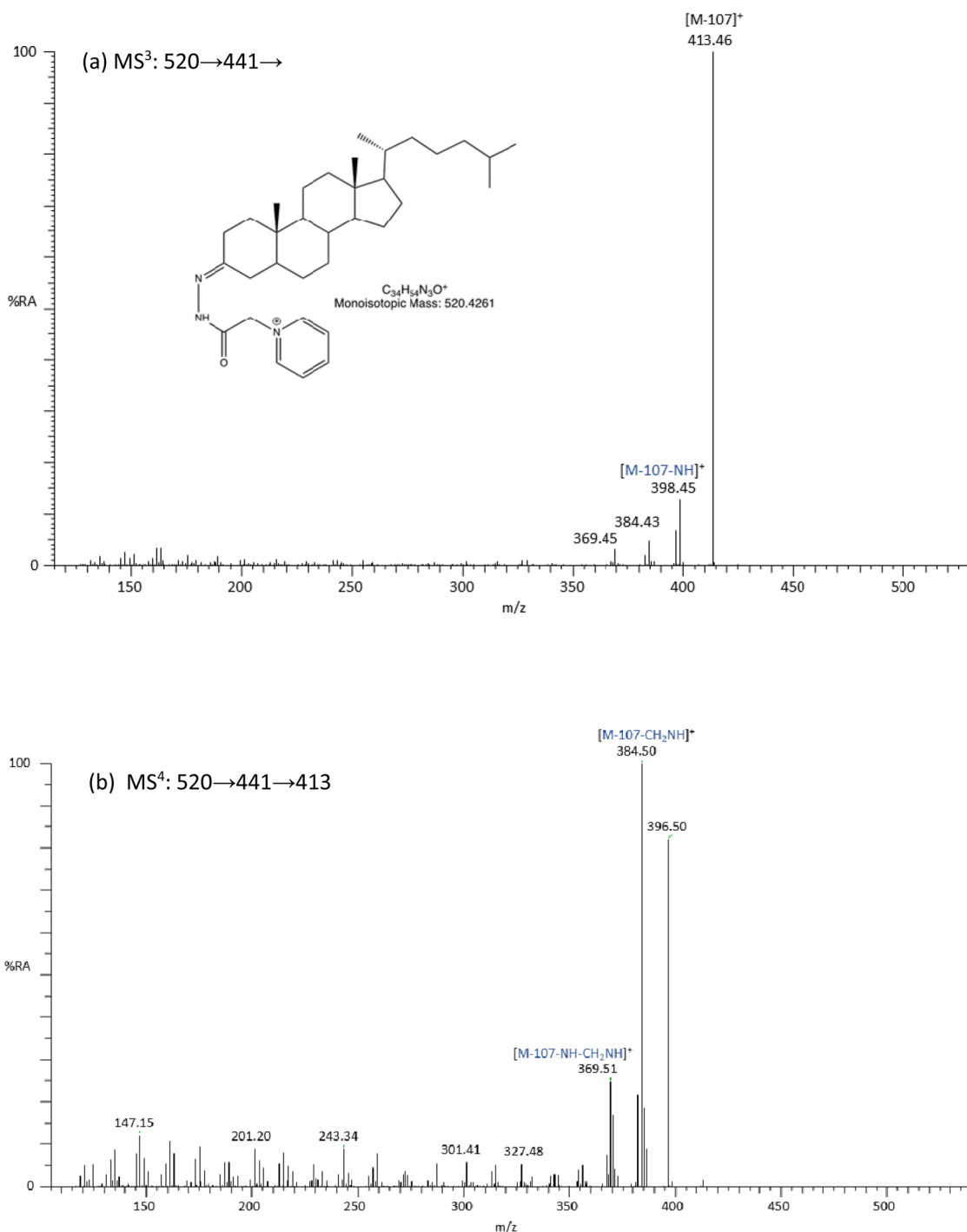


Fig. 7. (a) The MS³ (520.5→441.5→) spectrum, and (b) MS⁴ (520.5→441.5→413.5→) spectrum of O/GP-derivatised cholestanol authentic standard.

3.3. Identification of phytosterols in human serum

We adapted well validated protocol by Griffiths and colleagues [44, 46] for the extraction of oxysterols but we modified this protocol to include phytosterols. Briefly, phytosterols were extracted from microliter quantities of human serum using reversed-phase SPE cartridge (SPE-1 protocol), we found experimentally to fully elute phytosterols require SPE-1-Fr-1 9.5 mL of 70 % ethanol (an oxysterol-rich fraction), SPE-1-Fr-2 6 mL 99.9 % ethanol and SPE-1-Fr-3 2 mL dichloromethane (this solvent was evaporated and this fraction was reconstituted in SPE-1-Fr-7). SPE-1 fractions were then combined as one sample (Supplemental Figure S1), followed by enzyme assisted derivatisation for

sterol analysis (EADSA). EADSA consists of enzymatic conversion of 3 β -hydroxy-5-ene- and 3 β -hydroxy-5 α -hydrogen-containing sterols to 3-oxo-4-ene and 3-oxo sterols followed by derivatisation with GP hydrazine to their corresponding GP hydrazones (Fig. 2). To remove the excess of GP hydrazine further purification and fractionation was achieved using a recycling SPE-2 protocol using a reversed phase SPE cartridge. As the O/GP-derivatised phytosterols are more hydrophobic than the O/GP oxysterols, choleonic and cholestenoic acids, we determined experimentally to fully elute the O/GP derivatised cholesterol and phytosterols requires three 1-mL portions of 100 % methanol (SPE-2-Fr-1, 2, 3), four 1-mL portions of 99.9 % ethanol (SPE-2-Fr-4, 5, 6, 7) and two 1-mL portions of dichloromethane (SPE-2-Fr-8, 9)

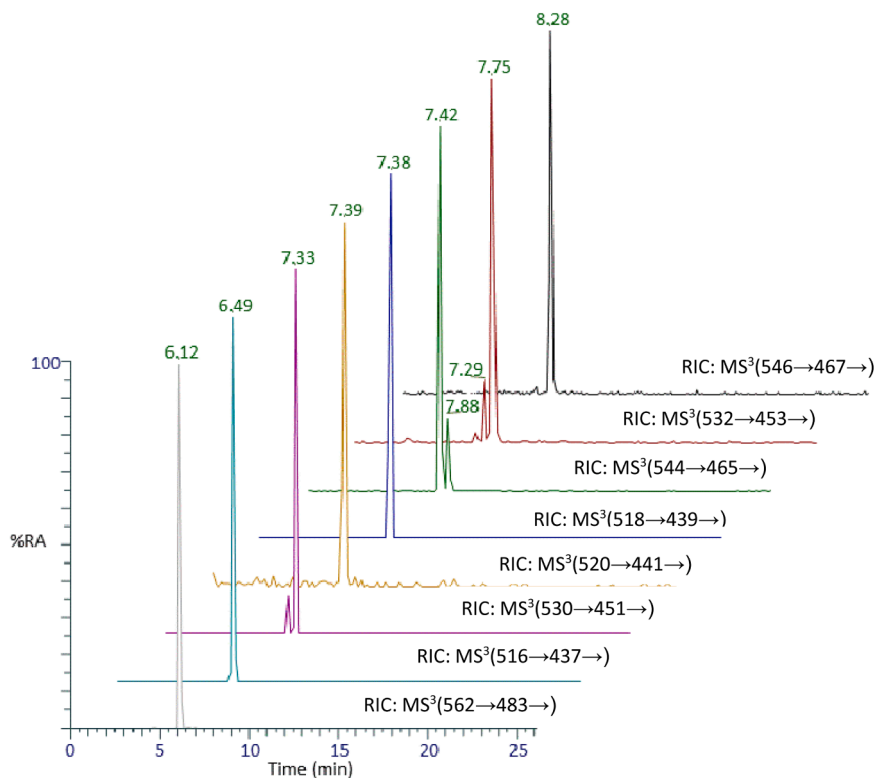


Fig. 8. LC-MS Reconstructed ion chromatograms (RICs) of MS^3 transitions ($[M]^+ \rightarrow [M-79]^+ \rightarrow$) of O/GP derivatised authentic standards corresponding to: (grey line) RT 6.12 min of the O/GP-7-oxo- β -sitosterol 562.5 \rightarrow 483.2 \rightarrow , (light green) RT 6.49 min of desmosterol 516.5 \rightarrow 437.5 \rightarrow , (purple) RT 7.33 min brassicasterol 530.5 \rightarrow 451.5 \rightarrow , (yellow) RT 7.39 min cholestanol 520.5 \rightarrow 441.5 \rightarrow , (blue) RT 7.38 min cholesterol and lathosterol 518.5 \rightarrow 439.5 \rightarrow , (green) RT 7.42 min fucosterol and 7.88 min stigmasterol 544.5 \rightarrow 465.5 \rightarrow , (brown) RT 7.75 min campesterol 532.5 \rightarrow 453.5 \rightarrow , (black) RT 8.28 min β -sitosterol 546.5 \rightarrow 467.5 \rightarrow .

(Appendix A). The direct infusion MS analysis revealed the GP-tagged oxysterols and already some phytosterols were present in the first 3 mL of methanol eluent (SPE-2-Fr-1, 2, 3), whereas GP-derivatised cholesterol, phytosterols were tailed into the SPE-2-Fr-4, 5, 6, 7 and to fully elute brassicasterol, stigmasterol, desmosterol required additional SPE-2-Fr-8 (1 mL of dichloromethane). Acidic sterols eluted predominantly in the first milliliter of methanol (SPE-2-Fr-1). GP-tagged hydrazones from each SPE-2 fractions were analysed separately and as combined aliquots of SPE-2-Fr-2, 3, 4, 5, 6, 7 fractions using the capillary LC coupled to the LTQ mass spectrometer. The identification of GP-tagged analytes was based on retention time (RTs) and MS^2 , MS^3 spectra comparison with authentic standards. In the absence of authentic standards, presumptive identifications were made based on a published library of MS^3 spectra for GP-sterols.

We analysed serum samples from two patients with AHC and JSLE and six healthy individuals and identified the O/GP derivatised cholesterol, cholesterol precursor desmosterol and five phytosterols fucosterol, campesterol, β -sitosterol, stigmasterol, brassicasterol in serum samples. An example of the O/GP derivatised fucosterol and stigmasterol identification is shown in Fig. 9 in serum sample from AHC patient. RIC of MS^3 (544.4 \rightarrow 465.4 \rightarrow) transition shows chromatographic peak at RT 7.42 and MS^3 spectrum was identical to the O/GP-derivatised authentic standard fucosterol (Fig. 5a), whereas an analyte eluted at RT 7.88 min was identified as the O/GP stigmasterol as its MS^3 spectrum was identical to the MS^3 spectrum of the authentic standard of O/GP-tagged stigmasterol (Fig. 5b). A ratio of fucosterol-to-stigmasterol in a healthy individual was around 1.25. Fig. 10a shows RIC for MS^3 (544.4 \rightarrow 465.4 \rightarrow) transition, the chromatographic peaks at RT 7.42 and 7.98 min were also assigned to the O/GP-tagged fucosterol and stigmasterol in the sample from AHC patient, the ratio of fucosterol-to-stigmasterol was 10. Two adults with AHC disorder showed an increased level of campesterol and β -sitosterol in comparison to healthy

individuals. AHC is a rare neurodevelopmental disorder that affects muscle movement and causes paralysis and muscle stiffness.

The following phytosterols: - campesterol, fucosterol and β -sitosterol were found in all serum samples, while stigmasterol and brassicasterol were only identified in around half of serum samples. As previously published campesterol and β -sitosterol are the most abundant phytosterols in serum [14,49]. For example, from the RIC for the MS^3 (516.5 \rightarrow 437.5 \rightarrow) transition shows three chromatographic peaks at RT 6.49, 6.73 and 7.09 min, which were in all serum samples (Fig. 10a). From the MS^3 spectra of the first two chromatographic peaks at RT 6.45 and 6.72 min, the presence of *b-series indicated there was no oxygen functionality on the B-ring of steroid skeleton (Fig. 10c) and RT of 6.49 min and MS^3 spectrum were identical to the O/GP-derivatised authentic standard of desmosterol. The chromatographic peak at 6.72 min did not match any literature libraries but this GP-derivatised sterol possibly corresponds to the O/GP-derivatised cholesta-5, x-dien-3 β -ol with double bond located on the side chain and an authentic standard required for positive identification (Fig. 10d). The analyte eluting at RT of 6.99 min was identified as a mixture of GP derivatised 7- and 8-dehydrocholesterol by comparison with the authentic standard MS^3 spectrum (Fig. 10e). Desmosterol and 7/8-dehydrocholesterol were identified in all samples.

The chromatographic peaks for MS^3 532 \rightarrow 453 \rightarrow transition at RT 5.58 min and 5.94 min (Fig. 10a) were assigned to the O/GP-derivatised cholest-4-ene-3,6-dione as GP-derivatised at C-3 and C-6 positions of the steroid ring (Figure S23) and at RT 7.74 min as campesterol based on their MS^3 spectra (Fig. 10a). For unknown GP-derivatised sterols for which we did not have authentic standards, we categorised them into two groups: - (a) with or (b) without *b-series fragment ions in their MS^3 spectra. The presence of *b-series was suspected to be sterols having no oxygen functionality on A or B ring [43]. The chromatographic peak at RT 6.88 min for RIC of MS^3 (530.4 \rightarrow 467.4 \rightarrow) transition (Fig. 10a) shows

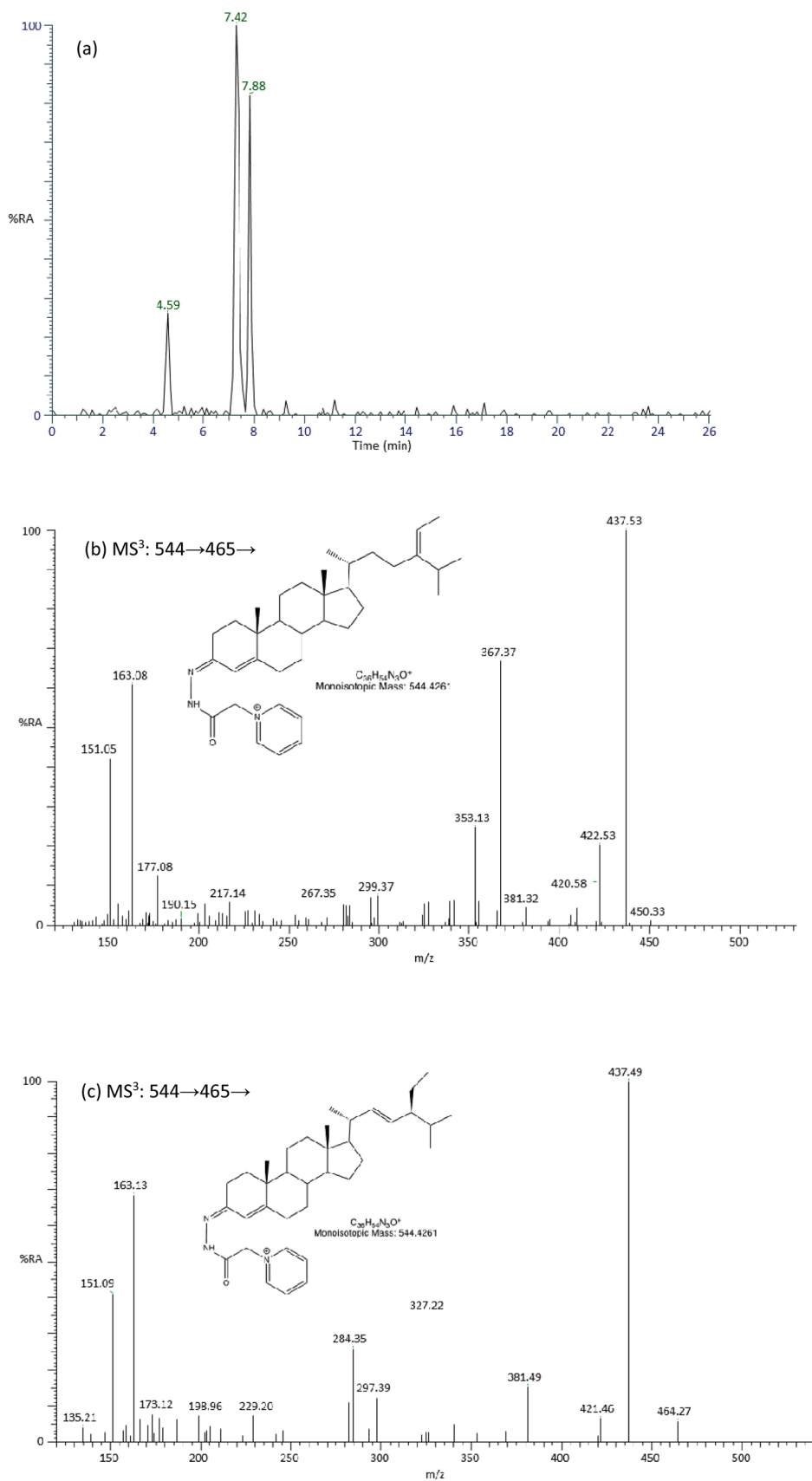


Fig. 9. LC-MS³ analysis using EADSA technology for serum sample from a healthy individual (a) RIC of MS³ (544.4→465.4→) transition, (b) The MS³ (544.4→465.4→) spectrum of the chromatographic peak at 7.42 min corresponding to fucosterol, (c) MS³ (544.4→465.4→) spectrum recorded at 7.88 min corresponding to stigmaterol as identified based on comparison of RTs and MS³ spectra with authentic standards.

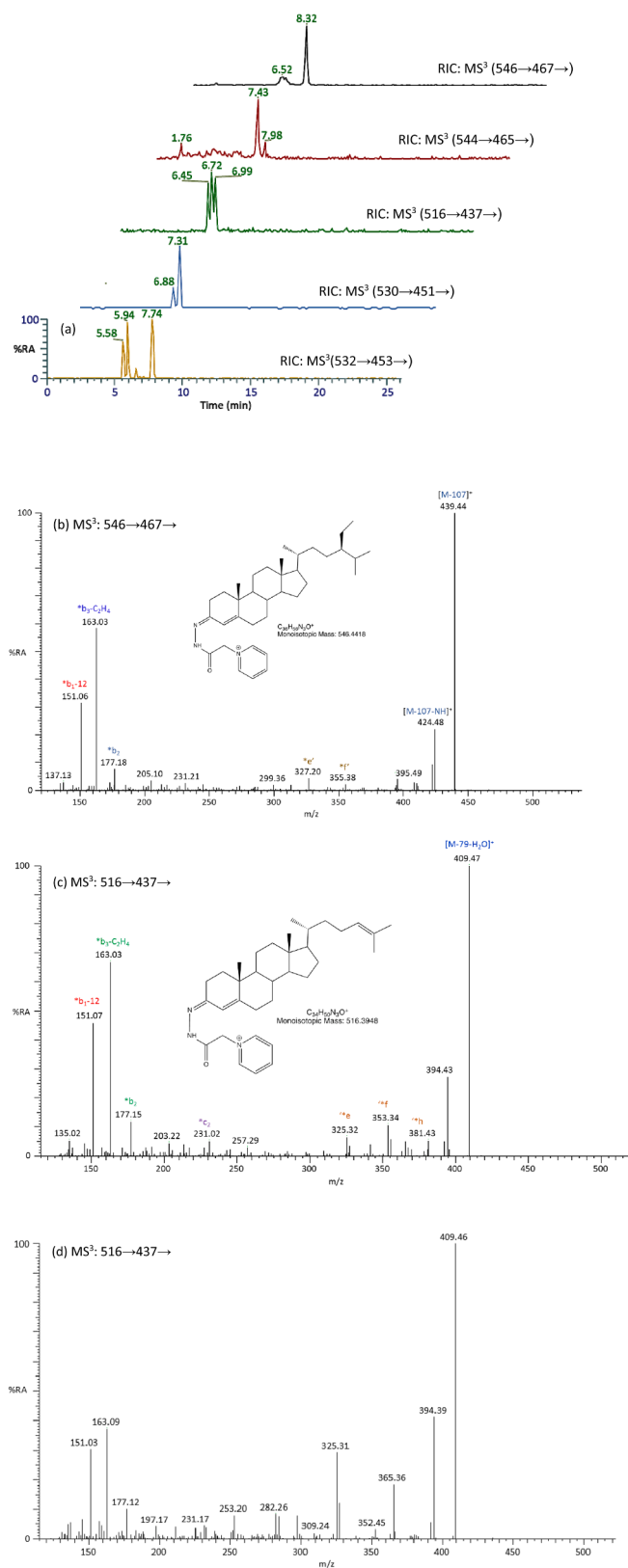


Fig. 10. (a) LC-MS RICS of MS^3 ($[M]^+ \rightarrow [M-79]^+$) transitions corresponding to GP-tagged phytosterols/sterols representative patient with AHC. The serum sample was subjected to the EADSA protocol. (b) The MS^3 (546.4 \rightarrow 467.4 \rightarrow) spectrum at RT 8.32 min assigned as sitosterol, (c) MS^3 (544.4 \rightarrow 465.4 \rightarrow) spectra at RT 7.43 min assigned to fucosterol and at RT 7.98 min to stigmasterol, MS^3 (516.4 \rightarrow 437.4 \rightarrow) shows three components eluted at (d) RT 6.45 min peak assigned as desmoterol and at RT 6.72 min possibly cholesta-5,x-dien-3 β -ol (with double bond on the side chain) and 7/8-dehydrocholesterol was assigned to the chromatographic peak at RT 6.99 min, (e) The MS^3 (530 \rightarrow 451 \rightarrow) spectrum at RT 7.31 min was brassicasterol, (f) the chromatographic peak at RT 7.75 min for the MS^3 (532 \rightarrow 453 \rightarrow) was identified as campesterol. The identifications were based on comparison of RTs and MS^3 spectra with authentic standards.

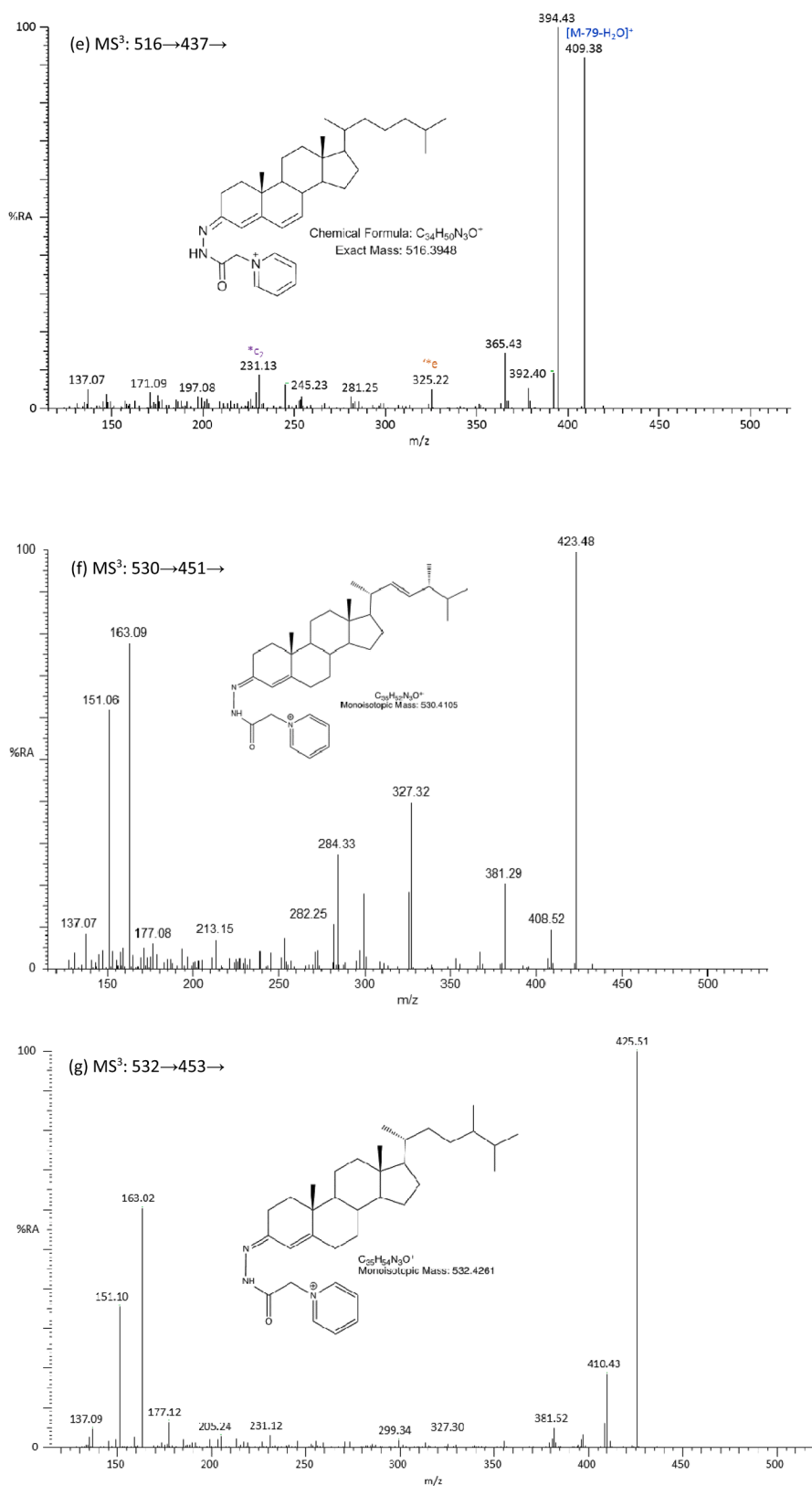


Fig. 10. (continued).

*b-series characteristic peaks at m/z 151, 163 and 177 possible a double bond in the sidechain at C17 which is built of nine carbons (Figure S23B), an authentic standard is required for a positive identification of this metabolite. The absence of *b-series fragments in MS^3 spectra were more likely to be sterols which have oxidation functionality

on A or B ring, therefore the B-ring cleavage is less prominent. Fig. 10a shows RIC for the transition of MS^3 (546.4 \rightarrow 467.4 \rightarrow) shows the chromatographic peak at RT 6.84 min corresponds to 3β -hydroxycholesta-5,7-dien-26-oic acid as identified by comparing with MS^3 spectrum [46] and at RT 8.32 min, MS^3 of which was identical to the O/GP-tagged

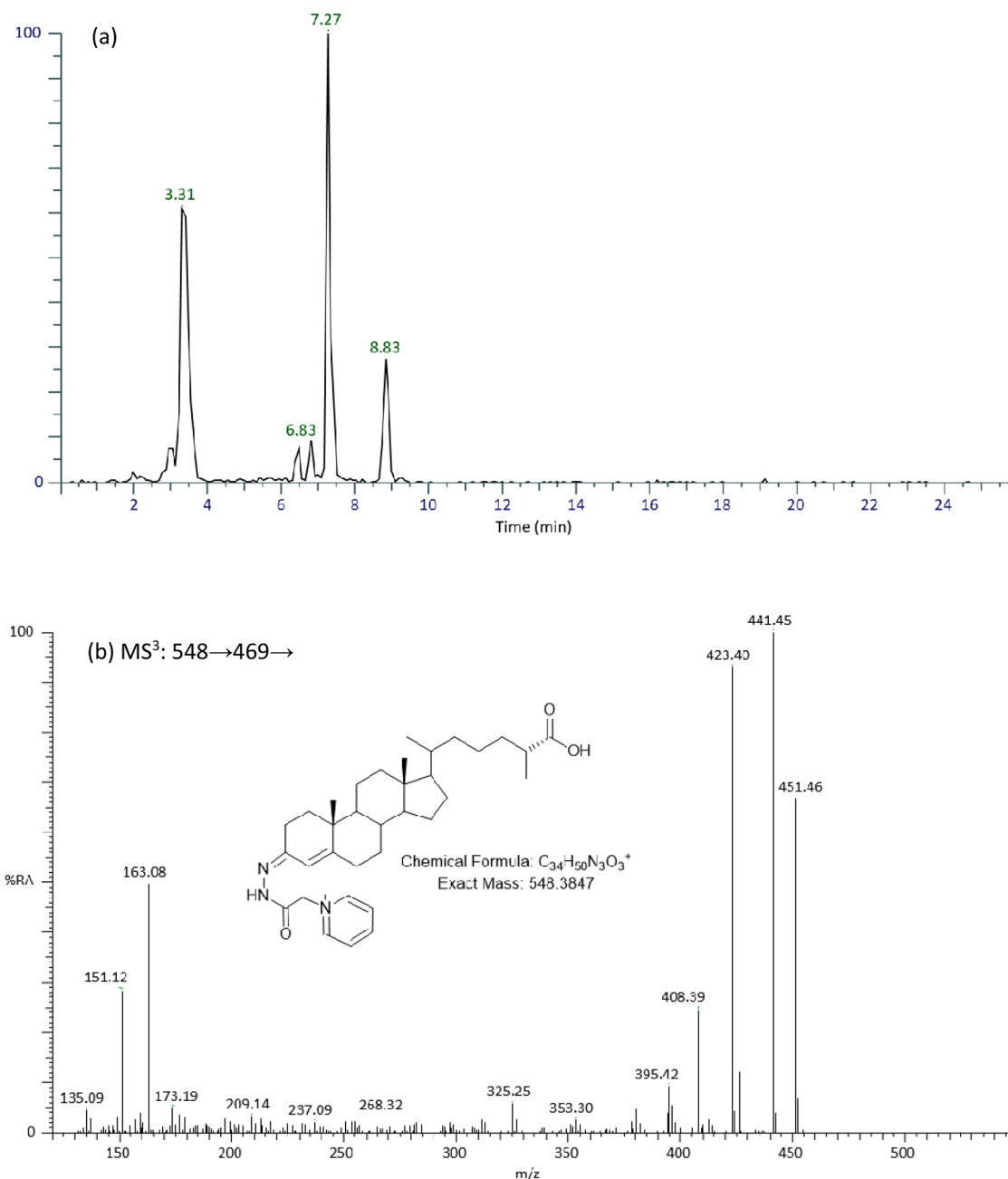


Fig. 11. (a) LC-MS RICs of MS³ (548→469→) transition corresponding to O/GP-sterols formed after EASDA protocol application using serum sample from an AHC patient. The MS³ (548→469→) spectrum of component eluting at (b) 3.31 min corresponding to 3β-hydroxycholest-(25R)-5-en-26-oic acid.

authentic standard of brassicasterol (Fig. 10b).

Several specific MS³ [M]⁺→[M-79]⁺ transitions were set up on the linear ion trap to search for 7-hydroxy and 7-oxo- containing phytosterols such as 7-oxo-campesterol and 7-hydroxy-campfigesterol ([M]⁺, *m/z* 548), sitosterol ([M]⁺, *m/z* 562), brassicasterol ([M]⁺, *m/z* 546), stigmasterol ([M]⁺, *m/z* 560), fucosterol ([M]⁺, *m/z* 560). 7-Oxo-phytosterols are a α,β-unsaturated ketone (5-en-7-one) and react with GP hydrazine in the absence of cholesterol oxidase enzyme. MS³ ([M]⁺→[M-79]⁺) fragmentation patterns for the 7-oxo derivatives differ from compounds with GP derivatisation at carbon position C-3 as shown for the 7-oxo-β-sitosterol (Fig. 6). The GP-derivatised 7-oxo-β-sitosterol was only measured in serum sample from a patient with AHC, the identification was based by RT and MS³ spectrum of authentic standard. Fig. 11 shows the RIC for 548→469→ transition, the chromatographic peak at 3.31 min corresponds to 3β-hydroxycholest-(25R)-

5-en-26-oic acid. The chromatographic peak at 7.27 min possibly 3β,5α,6α-trihydroxy-sterol, as MS³ spectrum shows a characteristic *b₂-ion at *m/z* 177 indication that sterol with a 3β-hydroxy group and a planar A/B ring system and an unusually prominent fragment-ion observed in the MS³ spectrum is at *m/z* 383 corresponding to [M-H₂O-79-72]⁺ (Figure S24A). The identity of analyte eluting from the C₁₈ column at RT 6.48, 6.83 and 8.83 min were not possible due to the absence of authentic standards (Figure S24B,C). There were also several oxysterols, cholestenic acid and unknown sterols measured in samples. The identification of some characterised and non-characterised sterols which followed a typical GP derivatised sterol fragmentation pattern ([M]⁺→[M-79]⁺) are summarised in Table S6. For those sterols not in our current library as an authentic standard, they were identified by MS³ ([M]⁺→[M-79]⁺) spectra comparison with published manuscripts using the EASDA technology combined with LC-MS³ analysis [23,41,44,

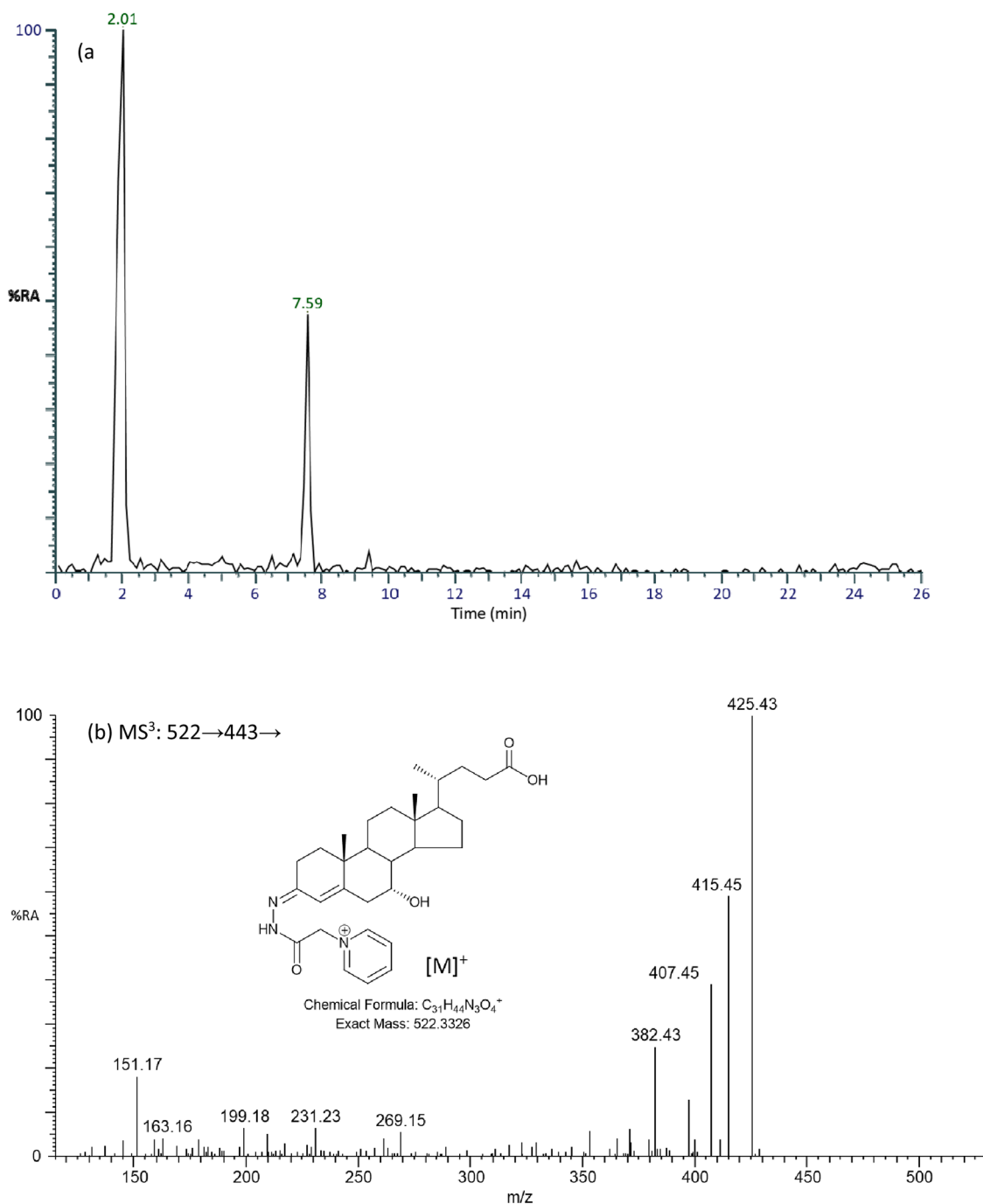


Fig. 12. (a) LC-MS RICs of MS³ (522→443→) transition, (b) MS³ spectrum recorded at 2.01 min corresponding to the O/GP derivatised 7 α -hydroxy-3-oxocholest-4-enoic acid.

47]. Most abundant sterols were also found in all samples and their RTs and MS³ spectra matched to cholest-4-ene-3,6-dione [43] (Figure S23), 3 β -hydroxy-5-cholestenoic acid [50], 7 α -hydroxy-3-oxo-4-cholestenoic acid [51], and 7 α -hydroxy-3-oxocholest-4-enoic acid [51] (Fig. 12a,b).

The chromatographic peaks at 1.37 and 1.75 min for the transition of MS³ (564.5→ 485.5→) correspond to 7 α -hydroxy-3-oxo-4-cholestenoic acid and 3 β ,7 α -dihydroxycholest-(25 R)-5-en-26-oic acid (Figure S25A and B) as they matched to MS³ from literature [21,41,47].

We analysed samples from patients with the autoimmune rheumatic disease juvenile-onset systemic lupus erythematosus (JSLE). Juvenile-onset SLE (JSLE) is a severe inflammatory disease that can affect any part of the body, and JSLE patients are known to have altered lipid metabolism, resulting in increased risk of cardiovascular disease [52,

53]. In JSLE, these changes in lipid metabolism and potentially oxysterol metabolism are linked to a strong type 1 interferon (IFN) signature [54]. Notably, Ch25h, a key rate limiting enzyme in metabolism of cholesterol into oxysterols, is an IFN-induced gene and changes in lipid profiles in patients with JSLE are associated with inflammation [55]. It has also been demonstrated that the expression of receptors of GPR183, whose main ligand is the oxysterol 7 α ,25-dihydroxycholesterol, are altered in immune cells in adult-onset SLE. Taken together, this strongly suggests that oxysterol profiles are likely to alter in JSLE when compared to controls. We utilised the published 21-min [46] gradient and our 26-min for chromatographic separation of hydroxycholesterols and dihydroxycholesterols (Figure S26). We identified the O/GP 7 α ,25-dihydroxycholesterol, 7 α ,27-dihydroxycholesterol, 24S-, 25-and

27-hydroxycholesterols in patients with JSLE and healthy individuals. This preliminary analysis suggests that there is a potential reduction in 25-hydroxycholesterol in JSLE serum compared to healthy control serum with more limited differences in 7 α ,25-dihydroxycholesterol (Figure S27). However, more *n*-numbers are needed to confirm these preliminary results.

4. Conclusion

Phytosterols have been supplemented in functional food products for their cholesterol-lowering ability, as well as other beneficial effects, leading to increased dietary exposure of both phytosterols and their oxidation products [3,13]. As a result, the physiological effects of phytosterols and oxidation products are constantly researched. Recent studies have suggested both phytosterols and oxyphytosterols can transverse the blood-brain-barrier and accumulate in the brain [13,20]. In this work, the EADSA method with a subsequent LC-MSⁿ analysis was applied for the analysis of non-esterified phytosterols in human serum. This method uses an extraction of phytosterols from serum, then sterols were oxidised with cholesterol oxidase enzyme and derivatised with Girard P reagent and analysed using a LC-MSⁿ. A library of authentic standards consisted of their retention time established on the C18 column and their corresponding MS, MS² and MS³ spectra was created and utilised for the identification of phytosterols in human serum. The LC-MSⁿ method was optimised for more hydrophobic sterols than cholesterol with a total LC run time of 26 min. The linear range was 0.2 pg/mL to 10 μ g/mL for campesterol, β -sitosterol and brassicasterol. The limit of quantification was 100 fg of the O/GP-tagged for brassicasterol and desmosterol as inject on the LC column. Phytosterols were semi-quantified using deuterated cholesterol as the internal standard. We found free campesterol serum concentration was in the range from 0.30 to 4.10 μ g/mL, β -sitosterol 0.16–3.37 μ g/mL, and fucosterol 0.05–0.38 μ g/mL in serum from 10 individuals (Table S5), and were in the same range as Lebecke J. and colleagues [56] reported free campesterol serum concentration in 49 individuals ranging from 0.55 to 4.73 mg/L and β -sitosterol from 0.32 to 2.29 mg/L those as determined using an APPI-LC-MS/MS methodology [56]. Plant J reported campesterol concentration is generally higher in serum than β -sitosterol [14]. Also, 7-oxo- β -sitosterol was identified in human serum based on its retention time and MS³ spectra. This methodology opens possibilities to investigate the role of phytosterols in human health and disease and could apply for the identification of oxyphytosterols in biological samples.

CRedit authorship contribution statement

Yu Chun Teng: Visualization, Validation, Methodology, Formal analysis, Data curation, Conceptualization. **Marie Claire Gielen:** Methodology, Formal analysis, Data curation. **Kersti Karu:** Writing – review & editing, Writing – original draft, Visualization, Validation, Supervision, Software, Resources, Project administration, Methodology, Investigation, Funding acquisition, Formal analysis, Data curation, Conceptualization. **Coziana Ciurtin:** Resources, Project administration. **Elizabeth C. Rosser:** Resources, Project administration. **Nina M De Gruijter:** Methodology, Investigation, Funding acquisition, Formal analysis, Data curation.

Data Availability

Data will be made available on request.

Acknowledgement

This work was supported by UCL Chemistry Department MSc in Applied Analytical Chemistry programme (to Y.C.T, M.C.G, K.K). NMDG was supported by a Medical Research Foundation Fellowship (MRF-057-

0001-RG-ROSS-C0797) awarded to ECR. ECR is supported by a Senior Research Fellowship from the Kennedy Trust for Rheumatology Research (KENN 21 22 09) and a Foundation for Research in Rheumatology (FOREUM) Research Career Grant (074) awarded to ECR. CC is supported by the National Institute of Health Research University College London Hospital Biomedical Research Centre (BRC4-III-CC). This work is also supported by a Versus Arthritis Centre for Excellence Grant awarded to Professor Lucy Wedderburn (21593) at the Centre for Adolescent Rheumatology Versus Arthritis at UCL, UCLH and GOSH. Kersti Karu is grateful to her PhD supervisors Professor William J. Griffiths and Professor Yuqin Wang (Swansea University Medical School, UK) for introducing/teaching her oxysterols and bile acids mass spectrometry analyses, and to collaborator at ThermoFisher Scientific in England, Mr Mark Sorenson. The authors thank Deepali Desai, Haoyi Minamiguchi and John Kakatsos for helping to generate figures and chemical structure drawings for this manuscript. Members of the European Network for Oxysterol Research (ENOR, <https://www.oxysterols.net/>) are thanked for informative discussions.

Appendix A. Supporting information

Supplementary data associated with this article can be found in the online version at [doi:10.1016/j.jsmb.2024.106519](https://doi.org/10.1016/j.jsmb.2024.106519).

References

- [1] J.N. Valitova, A.G. Sulkarnayeva, F.V. Minibayeva, Plant sterols: diversity, biosynthesis, and physiological functions, *Biochem. Moscow* 81 (8) (2016) 819–834.
- [2] T. Dierckx, J.F.J. Bogie, J.J.A. Hendriks, The impact of phytosterols on the healthy and diseased brain, *Curr. Med. Chem.* 26 (37) (2019) 6750–6765.
- [3] E. Hovenkamp, et al., Biological effects of oxidized phytosterols: a review of the current knowledge, *Prog. Lipid Res.* 47 (1) (2008) 37–49.
- [4] D. Lutjohann, et al., Sterol absorption and Sterol balance in Phytosterolemia evaluated by Deuterium-labeled Sterols - effect of Sitostanol treatment, *J. Lipid Res.* 36 (8) (1995) 1763–1773.
- [5] P.J.H. Jones, et al., Progress and perspectives in plant sterol and plant stanol research, *Nutr. Rev.* 76 (10) (2018) 725–746.
- [6] R.M. Alberici, et al., Rapid fingerprinting of sterols and related compounds in vegetable and animal oils and phytosterol enriched- margarines by transmission mode direct analysis in real time mass spectrometry, *Food Chem.* 211 (2016) 661–668.
- [7] H. Schaller, The role of sterols in plant growth and development, *Prog. Lipid Res.* 42 (3) (2003) 163–175.
- [8] H. Schaller, New aspects of sterol biosynthesis in growth and development of higher plants, *Plant Physiol. Biochem.* 42 (6) (2004) 465–476.
- [9] A. Schaeffer, et al., The ratio of campesterol to sitosterol that modulates growth in *Arabidopsis* is controlled by Sterol Methyltransferase 2;1, *Plant J.* 25 (6) (2001) 605–615.
- [10] T. Vanmierlo, et al., Plant sterols: friend or foe in CNS disorders? *Prog. Lipid Res.* 58 (2015) 26–39.
- [11] L. Baila-Rueda, et al., Simultaneous determination of oxysterols, phytosterols and cholesterol precursors by high performance liquid chromatography tandem mass spectrometry in human serum, *Anal. Methods* 5 (9) (2013) 2249–2257.
- [12] R.A. Moreau, et al., Phytosterols and their derivatives: structural diversity, distribution, metabolism, analysis, and health-promoting uses, *Prog. Lipid Res.* 70 (2018) 35–61.
- [13] F. Jie, et al., Linking phytosterols and oxyphytosterols from food to brain health: origins, effects, and underlying mechanisms, *Crit. Rev. Food Sci. Nutr.* 62 (13) (2022) 3613–3630.
- [14] J. Plat, et al., Plant-based sterols and stanols in health & disease: consequences of human development in a plant-based environment? *Prog. Lipid Res.* 74 (2019) 87–102.
- [15] L.M. Valsta, et al., Estimation of plant sterol and cholesterol intake in Finland: quality of new values and their effect on intake, *Br. J. Nutr.* 92 (2004) 671–678.
- [16] A. Jiménez-Escrig, A.B. Santos-Hidalgo, F. Saura-Calixto, Common sources and estimated intake of plant sterols in the Spanish diet, *J. Agric. Food Chem.* 54 (2006) 3462–3471.
- [17] S. Klingberg, et al., Food sources of plant sterols in the EPIC Norfolk population, *Eur. J. Clin. Nutr.* 62 (2008) 695–703.
- [18] R.E. Ostlund, et al., Gastrointestinal absorption and plasma kinetics of soy Delta (5)-phytosterols and phytostanols in humans, *Am. J. Physiol. Endocrinol. Metab.* 282 (4) (2002) E911–E916.
- [19] H. Gylling, P. Simonen, Phytosterols, Phytostanols, and Lipoprotein Metabolism, *Nutrients* 7 (9) (2015) 7965–7977.
- [20] M.M. Wang, B.Y. Lu, How do oxyphytosterols affect human health? *Trends Food Sci. Technol.* 79 (2018) 148–159.

- [21] K. Karu, et al., Nano-liquid chromatography-tandem mass spectrometry analysis of oxysterols in brain: monitoring of cholesterol autoxidation, *Chem. Phys. Lipids* 164 (6) (2011) 411–424.
- [22] H.F. Schött, D. Lütjohann, Validation of an isotope dilution gas chromatography-mass spectrometry method for combined analysis of oxysterols and oxyphytosterols in serum samples, *Steroids* 99 (2015) 139–150.
- [23] W.J. Griffiths, Y.Q. Wang, Cholesterol metabolism: from lipidomics to immunology, *J. Lipid Res.* 63 (2) (2022).
- [24] W.J. Griffiths, Y. Wang, Sterols, oxysterols, and accessible cholesterol: signalling for homeostasis, in immunity and during development, *Front. Physiol.* 12 (2021) 723224.
- [25] Y.Q. Wang, E. Yutuc, W.J. Griffiths, Cholesterol metabolism pathways - are the intermediates more important than the products? *Febs J.* 288 (12) (2021) 3727–3745.
- [26] R.E. Ostlund, Phytosterols and cholesterol metabolism, *Curr. Opin. Lipidol.* 15 (1) (2004) 37–41.
- [27] R.T. Ras, et al., Intake of phytosterols from natural sources and risk of cardiovascular disease in the European Prospective Investigation into cancer and nutrition-the Netherlands (EPIC-NL) population, *Eur. J. Prev. Cardiol.* 22 (8) (2015) 1067–1075.
- [28] J.C. Mathers, Plant foods for human health: research challenges, *Proc. Nutr. Soc.* 65 (2) (2006) 198–203.
- [29] W.J. Griffiths, P.J. Crick, Y. Wang, Methods for oxysterol analysis: Past, present and future, *Biochem. Pharmacol.* 86 (1) (2013) 3–14.
- [30] J.G. McDonald, et al., A comprehensive method for extraction and quantitative analysis of sterols and secosteroids from human plasma, *J. Lipid Res.* 53 (7) (2012) 1399–1409.
- [31] W.J. Griffiths, Y. Wang, Oxysterol research: a brief review, *Biochem. Soc. Trans.* 47 (2) (2019) 517–526.
- [32] G. Gachumi, A. El-Aneed, Mass spectrometric approaches for the analysis of phytosterols in biological samples, *J. Agric. Food Chem.* 65 (47) (2017) 10141–10156.
- [33] H.-F. Schött, D. Lütjohann, Validation of an isotope dilution gas chromatography-mass spectrometry method for combined analysis of oxysterols and oxyphytosterols in serum samples, *Steroids* 99 (2015) 139–150.
- [34] D.S. Mackay, et al., Methodological considerations for the harmonization of non-cholesterol sterol bio-analysis, *J. Chromatogr. B Anal. Technol. Biomed. Life Sci.* 957 (2014) 116–122.
- [35] G. Gachumi, A. El-Aneed, Mass spectrometric approaches for the analysis of phytosterols in biological samples, *J. Agric. Food Chem.* 65 (47) (2017) 10141–10156.
- [36] A. Honda, et al., Highly sensitive quantification of key regulatory oxysterols in biological samples by LC-ESI-MS/MS, *J. Lipid Res.* 50 (2) (2009) 350–357.
- [37] R. Sidhu, et al., A validated LC-MS/MS assay for quantification of 24(S)-hydroxy-cholesterol in plasma and cerebrospinal fluid, *J. Lipid Res.* 56 (6) (2015) 1222–1233.
- [38] E. Yutuc, et al., Deep mining of oxysterols and cholestenic acids in human plasma and cerebrospinal fluid: Quantification using isotope dilution mass spectrometry, *Anal. Chim. Acta* 1154 (2021) 338259.
- [39] W.J. Griffiths, et al., New methods for analysis of oxysterols and related compounds by LC-MS, *J. Steroid Biochem. Mol. Biol.* 162 (2016) 4–26.
- [40] H. Hong, Y. Wang, Derivatization with girard reagent T combined with LC-MS/MS for the sensitive detection of 5-Formyl-2'-deoxyuridine in cellular DNA, *Anal. Chem.* 79 (1) (2007) 322–326.
- [41] W.J. Griffiths, et al., Analysis of oxysterols by electrospray tandem mass spectrometry, *J. Am. Soc. Mass Spectrom.* 17 (3) (2006) 341–362.
- [42] W.J. Griffiths, et al., Analytical strategies for characterization of oxysterol lipidomes: liver X receptor ligands in plasma, *Free Radic. Biol. Med.* 59 (2013) 69–84.
- [43] K. Karu, *Anal. Oxysterols Capill. Liq. Chromatogr. Tandem Mass Spectrom.* (2009).
- [44] W.J. Griffiths, et al., Analytical strategies for characterization of oxysterol lipidomes: liver X receptor ligands in plasma, *Free Radic. Biol. Med.* 59 (2013) 69–84.
- [45] W.J. Griffiths, et al., The cerebrospinal fluid profile of cholesterol metabolites in Parkinson's disease and their association with disease state and clinical features, *Front Aging Neurosci.* 13 (2021) 685594.
- [46] E. Yutuc, et al., Deep mining of oxysterols and cholestenic acids in human plasma and cerebrospinal fluid: quantification using isotope dilution mass spectrometry, *Anal. Chim. Acta* 1154 (2021) 338259.
- [47] Y.Q. Wang, et al., Targeted lipidomic analysis of oxysterols in the embryonic central nervous system, *Mol. Biosyst.* 5 (5) (2009) 529–541.
- [48] A.L. Dickson, et al., Identification of unusual oxysterols biosynthesised in human pregnancy by charge-tagging and liquid chromatography - mass spectrometry, *Front. Endocrinol.* 13 (2022) 1031013.
- [49] T. Vanmierlo, et al., The plant sterol brassicasterol as additional CSF biomarker in Alzheimer's disease, *Acta Psychiatr. Scand.* 124 (3) (2011) 184–192.
- [50] Dickson, A., et al., HSD3B1 is an Oxysterol 3 β -Hydroxysteroid Dehydrogenase in Human Placenta. *bioRxiv*, 2022: p. 2022.04.01.486576.
- [51] Dickson, A.L., et al., Identification of Unusual Oxysterols Biosynthesised in Human Pregnancy by Charge-Tagging and Liquid Chromatography - Mass Spectrometry. *bioRxiv*, 2022: p. 2022.02.07.478301.
- [52] G.A. Robinson, et al., Increased apolipoprotein-B:A1 ratio predicts cardiometabolic risk in patients with juvenile onset SLE, *Ebiomedicine* 65 (2021).
- [53] E.M.D. Smith, et al., Juvenile-onset systemic lupus erythematosus: update on clinical presentation, pathophysiology and treatment options, *Clin. Immunol.* 209 (2019).
- [54] M.J. Wahadat, et al., Type I IFN signature in childhood-onset systemic lupus erythematosus: a conspiracy of DNA- and RNA-sensing receptors? *Arthritis Res. Ther.* 20 (2018).
- [55] G.A. Robinson, et al., Metabolomics defines complex patterns of Dyslipidaemia in Juvenile-SLE patients associated with inflammation and potential cardiovascular disease risk, *Metabolites* 12 (1) (2022).
- [56] J. Lembcke, et al., Rapid quantification of free and esterified phytosterols in human serum using APPI-LC-MS/MS, *J. Lipid Res.* 46 (1) (2005) 21–26.